R. & M. No. 3252

MINISTRY OF AVIATION

AERONAUTICAL RESEARCH COUNCIL
REPORTS AND MEMORANDA

Turbulent Wall Jets with and without an External Stream

By P. BRADSHAW, B.A. and M. T. GEE, B.Sc.
OF THE AERODYNAMICS DIVISION, N.P.L.

LONDON: HER MAJESTY'S STATIONERY OFFICE
1962
PRICE: £1 0s. 0d. NET

Turbulent Wall Jets with and without an External Stream

By P. Bradshaw, B.A. and M. T. Gee, B.Sc.
of the Aerodynamics Division, N.P.L.

*Reports and Memoranda No. 3252**
June, 1960

Summary. The results are presented of experiments on wall jets in still air on flat and curved surfaces, and beneath an external stream in presence and absence of pressure gradient and initial boundary layer. It is found that the Reynolds shear stress is not zero at the velocity extrema, invalidating the simple assumptions of layer independence made by other workers: it is concluded that a satisfactory calculation method is not immediately practicable. The behaviour of wall jets is discussed in some detail on the basis of the experimental results.

1. *Introduction.* The behaviour of jets blowing tangentially to a solid surface has recently become of interest partly because of a theoretical solution for the wall jet in still air by Glauert[1] supported by the experiments of Bakke[2] and Sigalla[3,4] and partly because of the use of tangential jets for aircraft boundary-layer control. Previous literature on the subject is scattered: Sigalla[3] refers to several little-known studies including the work of Förthmann[5] in 1934. The analysis of the laminar jet by Tetervin[6], who obtains results in good agreement with Glauert's, should also be mentioned, but is of little practical interest in view of the extremely low critical Reynolds number of mixing layer flows. The simpler related problem of a free jet blowing parallel to an (accelerating) stream has been studied by Squire[7], Abramovich[8] and others.

A wall jet mean velocity profile is typically a half-jet with an inner wall layer, and Glauert[1] found that a near-similarity solution for the turbulent case could be obtained by assuming that the variation of shear stress with mean velocity was the same as that in turbulent pipe flow inside the velocity peak, while outside the velocity peak a constant eddy viscosity was assumed, the value being chosen to obtain a velocity profile in agreement with Bakke's experiments on the radial wall jet. These assumptions have the corollary that the shear stress is zero at the velocity peak, and it was found from the analysis that the shapes of the wall layer and mixing layer profiles were to a very good approximation independent of their relative length scales, indicating that the interaction between the two parts of the flow was very small, an expected result of the hypothesis. Sigalla studied the two-dimensional wall jet and obtained an eddy viscosity flow constant which differed both from Bakke's value and from the value in a two-dimensional free jet: he also measured surface friction with Preston tubes and deduced a law similar to the Blasius law assumed by Glauert but with a factor 25 per cent greater. On making the appropriate modification to the numerical results of Glauert's theory, good agreement with his predictions of mean velocity profile was again obtained.

* Previously issued as A.R.C. 22,008.
Published with the permission of the Director, National Physical Laboratory.

Experiments to date therefore support Glauert's theory qualitatively and, with the above reservations, quantitatively.

Little study bearing on the present problem has been made of the jet blowing over a curved surface in still air. The continued attachment of the jet to the surface is the well-known 'Coanda effect', but such experiments as have been made, for instance those of Gates[9] have dealt chiefly with the overall features of the flow rather than with the shear layer development. Ref. 9 gives an extensive bibliography. The interest in this problem lies in its possible relation to the flow near the knee of a blown flap and to certain deflected-stream schemes for high lift, in the alleged mystery of the Coanda effect itself, and in the general question of the effect of streamwise curvature on turbulent flow.

Much work has been done on tangential blowing for aircraft boundary-layer control, but most of it has been of an *ad hoc* nature intended to determine the performance of given types of aircraft configuration, and, at the time of writing, the only published researches contributing specifically to the understanding of the blown flap as a boundary layer phenomenon seem to be those of Carrière *et al*[10]. These authors give results of mean velocity profile traverses in a jet blowing tangentially beneath the boundary layer on a wind tunnel wall and on the deflected flap of an aerofoil, and also present a step-by-step calculation method in which the profile is divided into layers between the velocity extrema, each layer being treated separately with the aid of empirical formulae for eddy viscosity and surface friction.

The present investigation was planned to explore the mean velocity and turbulent intensity profiles in the wall jet both in still air and beneath an external stream, paying particular attention to the mixing of a wall jet with a boundary layer and the effect of pressure gradient. It was hoped that a calculation method could be devised to enable the development of the flow over an aircraft blown flap to be predicted, although it was appreciated that such a complicated flow would have to be treated by an extension of the existing empirical calculation methods for the turbulent boundary layer rather than by an elegant method like that of Glauert, as it appeared unlikely that there was any simple relation linking the various parts of the flow. No attempt was made in the experiment to study the effect of permutation of the many available parameters: the intention was to derive as much information as possible in physical terms in preference to empirical formulae.

A preliminary experiment on the two-dimensional wall jet blowing over a flat surface in still air was designed because at that time the only available wall jet data were given in the experiments of Bakke on a radial wall jet and it was felt that knowledge of the behaviour of a two-dimensional wall jet was a necessary preliminary to a study of the blown flap. It was also intended to extend Bakke's data by measuring surface friction and turbulence.

A similar investigation of the flow over a curved surface was made partly because of the aforementioned case of the blown flap knee and partly because of the controversy about the causes of 'Coanda effect'.

The next arrangement to be studied was the mixing of a wall jet with a constant-velocity external stream. In this case, profile similarity cannot be even approximately satisfied as the ratio of jet peak velocity to mixing layer edge velocity, which is constant (infinite) in the still air case, changes continuously from a large value near the nozzle to unity when the jet peak just disappears. Consequently, the characteristics of the mixing layer will change from those of a jet to those of a wake. After this, mixing with a boundary layer, still in zero pressure gradient, was investigated to see if further new phenomena resulted from a varying velocity at the outer edge of the mixing layer as well as the inner edge.

Finally an experiment was made on the wall jet mixing with a boundary layer in an adverse pressure gradient on the deflected rear flap of a two-dimensional aerofoil, combining the effects investigated separately above in a model of the aircraft blown flap.

It was hoped that the experimental information thus obtained would throw light on the factors which control the flow, enabling a qualitative description to be obtained, and also provide enough quantitative information to permit the development of a calculation method, preferably based as much as possible on physical arguments and assumptions reinforced by empirical formulae. In fact, the most obvious simple assumption which could be made, that the flow can be divided into layers each having the properties of some known type of shear flow, proved to be invalid, and it has not yet been possible to derive any other simple method with reasonably plausible assumptions giving accurate results because of the strong interactions of the various parts of the flow which render impracticable any 'multi-layer' analysis of the type here envisaged. However, much useful information about the flow over a blown flap has been obtained; the conclusions are summarised in Section 5.

2. *Apparatus and Measurement Techniques.* The apparatus used is shown in Fig. 1. The tests were conducted on the surface of a crude aerofoil, whose top surface was flat except at two hinge lines fore and aft where flaps were attached. Both flap angles could be varied, and the length of the rear flap could be altered by adding or removing sections. In addition, the rear flap could be replaced by a semi-circular cylinder of radius 9 in. which was used for the experiments on the 'Coanda effect'. For the measurements with an external stream the aerofoil was mounted vertically between end plates in the N.P.L. 9 ft × 7 ft No. 2 Tunnel. Tunnel speeds ranged up to about 120 ft/sec: the zero pressure gradient runs were all made at a free-stream Reynolds number of $5 \cdot 88 \times 10^4$ per in. (110 ft/sec nominal), and the adverse pressure gradient runs at $5 \cdot 17 \times 10^4$ per in. A blowing duct was fitted at the rear hinge line, and static pressure tappings were fitted at frequent chordwise intervals.

Two blowing ducts were used. The first was a tube of 2 in. diameter with a slot nominally 0·018 in. high and a lip of about 0·01 in. thickness. Spacers were fitted at 2 in. intervals in the mouth of the slot. The spanwise distribution of exit velocity and mass flow was poor: a wake existed behind each spacer and there were also random spanwise variations of ± 15 per cent in velocity. By choosing a region where the velocity was reasonably constant for several inches spanwise, the still-air and zero pressure gradient work (with the exception of the hot wire measurements which were made later) was satisfactorily completed, but early attempts at measurement in adverse pressure gradient were unsuccessful since the flow was far from parallel to the free-stream direction and tended to change with time, evidently owing to a combination of lip deflection and dust accretion, both accentuated by the narrowness of the slot. This problem of spanwise uniformity has arisen in many flap-blowing experiments, aggravated by the need for a small duct with a thin lip to the blowing slot, but able to stand high internal pressures without distortion. A new blowing duct was therefore made: the duct itself was of rectangular section, and the blowing slot was 0·040 in. high with a 0·050 in. lip. Spacers were fitted every 3 in. except for a 6 in. gap near the measurement chordline. The spanwise distribution of velocity was much more satisfactory and the tests in adverse pressure gradient were then successfully completed. The chief shortcoming of this duct was a spanwise component of exit velocity which resulted in premature separation from one end plate when a very long deflected flap was used. This asymmetry occurred primarily because this duct, like its

predecessor, was fed from one end only, but it is likely that a (symmetrically distributed) lateral velocity component would still exist with injection from both ends. Problems of blowing duct design have been discussed by Butler and Williams[11]. The air was supplied from the Aerodynamics Division 350 p.s.i. storage bottles through a series of pressure reducers: the arrangement used was similar to that shown in Fig. 2 of Ref. 12. The mass flow was calculated from orifice plate readings but these proved insufficiently sensitive for day-to-day running and the pressure difference between two tappings in the blowing duct, one on the floor and one on the lower lip of the slot, which was closely equal to the jet dynamic pressure, was used instead. The slot exit velocities used were about 650 ft/sec in the case of the 0·018 in. slot and 350 ft/sec for the 0·040 in. slot: it was decided that although sonic nozzles would almost certainly be used on aircraft blown flaps, the data required in this experiment could be equally well obtained in subsonic flow.

Remotely-controlled traverse gear for velocity traverses could be inserted from the lower surface through holes in the flap sections or the cylinder but for traverses near the slot it was necessary to mount the jack on a gantry attached to the tunnel wall: interference with the flow was checked and found to be negligible. The $3\frac{1}{2}$ in. diameter discs carrying the skin friction surface tubes could be inserted in the flap at two positions approximately 13 in. and 25 in. from the slot.

Mean velocity traverses were made with flattened pitot tubes of about 0·01 in. height. Surface friction was measured with surface pitot tubes as described in Ref. 13. Turbulence measurements were made using 0·0002 in. dia. platinum-rhodium hot wires. The electronic apparatus, purchased from Dr. G. Dätwyler of Zurich, is a constant-current set with resistance-inductance compensation and a square wave generator for setting the wire time constant. The -3db points at which the amplifier gain falls to $1/\sqrt{2}$ of its nominal value are about 3 c.p.s. and 30 kc.p.s.

No corrections have been made for the effect of turbulence or probe angle of attack on the pitot and static tube pressures. The resulting errors are serious only in the outer part of the still-air jet where the turbulence is very high and, owing to entrainment, the mean streamline inclination to the surface is considerable: the still air mean velocity profiles, as a result, appear almost linear from $U = 0{\cdot}5U_j$ to $U = 0$, and beyond the latter point negative dynamic pressures were observed —but not recorded—indicating that the crossflow angles were at least 45 deg. The correction to be applied to pitot tube readings has been given by Goldstein[14] as

$$\tfrac{1}{2}\rho U^2 = P - p - \tfrac{1}{2}\rho(\tilde{u}^2+\tilde{v}^2+\tilde{w}^2)$$

but it ceases to be valid in high-intensity turbulence where $\tan^{-1} v/(U+u)$, the instantaneous crossflow angle, may differ greatly from zero, and even exceed 90 deg, causing the pitot tube to read low. In addition, Westley[15] has shown that pitot tubes and manometers may possess resonant frequencies within the usual range of turbulent eddies so that the response becomes a complicated function of the turbulence spectrum: however this last effect should not be too important with fine pitots at low speeds as in the present experiment. In view of these great uncertainties about the corrections to be made, and since none had been made by the experimenters with whose results it was desired to make comparison, it was decided to ignore them. Further remarks on the use of pressure tubes in turbulent jets and separated flows have been made by Johannesen[16], and Garner and Walshe[17].

The turbulence measurements are susceptible to error on account of the non-linear response of the wire, but again the errors should be gross only in the outer part of the free jet, where the R.M.S. longitudinal component of turbulence exceeds 30 per cent of the mean velocity. Only a linearized hot-wire anemometer is capable of giving accurate results in high intensity turbulence.

Most of the measurements of mean speed and turbulence have been satisfactorily repeated. An exception is the single set of turbulence readings in the wind tunnel which were not checked because the tunnel air was so impossibly dirty that hot wire measurements were abandoned. Nevertheless the readings are included as a matter of interest, and seem to vary in a reasonable manner. All the turbulence measurements were made in the early stages of revival of hot wire work at N.P.L. and are not to be regarded as definitive: it is hoped, however, that the data are not greatly in error as satisfactory agreement has been obtained with the results of Laufer[18] in a series of check measurements in a circular pipe.

3. *Results.* The results are shown in the figures, which are arranged in the order in which they are referred to in the discussion which follows.

4. *Discussion.* The discussion is divided into sections dealing with each arrangement tested and it is convenient to comment on the various phenomena with reference to the particular flows in which they were actually observed, but many of the remarks made about the behaviour of the still air wall jet also apply to the cases with an external stream. We shall refer to the region between the surface and the position of the velocity maximum (*see* Fig. 2) as the 'wall layer', and to the region beyond the velocity maximum as the 'jet layer'. The terms 'inner layer' and 'outer layer' will be used to denote the hypothetical similarity regions in the wall layer, regarding the latter as a boundary layer.

4.1. *Wall Jet in Still Air on a Flat Surface.* The results for mean velocity profiles (Fig. 2), shear layer streamwise development (Fig. 3) and surface friction (Fig. 4) agree quite well with those of Sigalla[4] which as already remarked are in general agreement with Glauert's theory, and seemed at first sight to justify his hypothesis that the profile could be divided at the velocity peak into two layers for purposes of calculation. The jet layer profiles coincide with Glauert's to within the limits of experimental accuracy though it is of course well known that all free shear layer profiles are nearly geometrically similar.

The Flow Constant for the Jet Layer. Glauert's flow constant for the jet layer, $\mathscr{K} \equiv \nu_T/U_j\delta_{0\cdot5}$, was chosen, on the strength of Bakke's experiments, as $0\cdot012$ in order to make the profile shape agree with theory: alternatively one may calculate the flow constant from the observed rate of growth of the jet layer. Applying the two methods to the case of the two-dimensional wall jet (using Sigalla's results for convenience since he has made a direct comparison between his profiles and the theory and since his surface friction law—though the numerical values agree quite well with the present results—retains the slope $-1/4$ on which Glauert's theory was based rather than the slope $-0\cdot18$ which gives the best fit to the present results) we obtain respectively $\mathscr{K} = 0\cdot0136$ and $\mathscr{K} = 0\cdot0124$, a disagreement of 10 per cent which is satisfactory in view of the sensitivity of $\mathscr{K}$ to $\delta_j/\delta_{0\cdot5}$: the error corresponds to an error of about 10 per cent in determining $\delta_j/\delta_{0\cdot5}$ which is quite a likely value in view of the flat-topped nature of the profile, so that substantiation of the theory appears to be good.

The Velocity Profile in the Wall Layer. A discrepancy occurs between the wall layer velocity profiles: the results of Bakke and Sigalla were obtained with rather large pitot tubes and the authors attributed the low velocities (compared with theory) observed near the wall to instrument error. The present results (Fig. 5), obtained with pitot tubes typically 5 per cent of the height of the wall layer, show higher velocities than those predicted by Glauert's theory for a given value of y/δ_j,

but if one plots the theoretical and experimental profiles in the form U/u_τ against $u_\tau y/\nu$ (or its logarithm), using the Blasius skin friction formula for Glauert's results and choosing $U_j\delta_j/\nu = 10^4$, one obtains fairly good agreement between the two (Fig. 6). Glauert's 'inner law' is not quite a semi-logarithmic one, as far as can be seen from values taken from his graphs, but a reasonable straight-line fit in the usual inner law region is

$$\frac{U}{u_\tau} = 4{\cdot}7 \log \frac{u_\tau y}{\nu} + 6{\cdot}8 = 16{\cdot}2 \text{ when } \frac{u_\tau y}{\nu} = 100$$

compared with the usual circular pipe law

$$\frac{U}{u_\tau} = 5{\cdot}75 \log \frac{u_\tau y}{\nu} + 5{\cdot}5 = 17 \quad \text{when } \frac{u_\tau y}{\nu} = 100$$

The two laws coincide to within about 5 per cent on velocity or 10 per cent on surface friction. If one substitutes Sigalla's experimental surface friction formula in Glauert's theoretical profile, the resultant inner law is very different from the pipe or boundary-layer laws: this is odd, because Glauert's equation for the profile does not involve the constant term in the surface friction formula so that one would not necessarily expect the resultant inner law to follow the pipe law using Blasius' surface friction formula rather than any other. The explanation appears to be that Glauert incorporated pipe data in the hidden form of the assumption of a 1/7 power law velocity profile near the wall, thus ensuring that the inner law would be

$$\frac{U}{u_\tau} = \frac{1}{k^{4/7}} \left(\frac{u_\tau y}{\nu}\right)^{1/7}$$

where

$$\tau_0 = k\rho U_j^2 \left(\frac{U_j\delta_j}{\nu}\right)^{-1/4}$$

The Blasius value of k, $0{\cdot}0225$, gives an inner law which agrees very well with the pipe law, but Sigalla's value for k, 25 per cent greater, gives quite a different result.

Doubtful Applicability of the Overlap Law Assumption. In view of the approximations and assumptions made in Glauert's method one would not expect an exactly semi-logarithmic inner law to appear: however the observation that the *experimental* inner law is not semi-logarithmic, leads one to doubt the validity of the inner law and defect law overlap assumptions in this case, particularly as one would expect the semi-logarithmic part of the graph to have a gradient of between 5 and 6—roughly $\log_e 10$ times the reciprocal of von Kármán's constant—whereas the experimental curve has this gradient only at about $u_\tau y/\nu = 30$, the lower boundary of the usual inner law.

The usual prediction of a semi-logarithmic inner law is obtained from the hypothesis that the inner law

$$\frac{U}{u_\tau} = f\left(\frac{u_\tau y}{\nu}\right)$$

and the defect law

$$\frac{U_1 - U}{u_\tau} = g\left(\frac{y}{\delta}\right)$$

overlap for an appreciable distance, whence it can be shown (for instance by equating the expressions for the velocity gradient in the overlap region obtained from the two laws) that f and g must be

logarithmic functions in the overlap region. The semi-logarithmic region is not very large at low Reynolds numbers, but one would expect to be able to identify it clearly in a boundary layer at $R_\delta = 10^4$.

Although the range of test Reynolds numbers was limited it seems fairly certain that there is a true inner law with no tendency to change with Reynolds number: the inner profiles fall closely together even though the jet layer profiles beyond the velocity peak diverge rapidly. In view of the independence hypothesis and similarity of profiles one would also expect there to be a defect law, extending outwards at least as far as the peak, which would vary only slowly with the Reynolds number and the ratio of wall layer to jet layer width which is a function of Reynolds number. Although this is not confirmed very well by the defect law plots (Fig. 7) based on δ_0, the distance from the surface at which $(U_j - U)/u_\tau = 1$, the deviations do not seem well correlated with the Reynolds number (except of course very near the wall) so that in default of better data one must take this as a fair indication of the presence of a defect law.

Evidence for Interaction between the Wall and Jet Layers. If, therefore, there exist both inner and defect laws one would definitely expect a perceptible semi-logarithmic region in the layer, with a law approximating to that in the pipe or the boundary layer, and its absence is strong evidence that the layer independence assumption is incorrect, and that the jet layer profile is influencing the wall layer to such an extent that the defect law is no longer the simple $(U_j - U)/u_\tau = g(y/\delta)$ but a more complicated function involving $\delta_j/\delta_{0\cdot5}$, U_j/u_τ or the Reynolds number (which all amount to the same thing since they are almost certainly simply related). Admittedly this is not explicitly confirmed by the experimental results mentioned above, but the ratio of the largest Reynolds number to the smallest was only 2:1 which is probably insufficient to show up any deviation of the sort suggested. The experiments are hampered by the fact that the local Reynolds number varies only as $x^{1/2}$. The alternative explanation is that the two laws *do* exist but do not overlap appreciably. In view of the fact that the inner law seems to extend to about $\log u_\tau y/\nu = 2\cdot2$, this is improbable.

Finite Shear Stress at the Velocity Peak. More definite evidence of interaction, and incidentally the overthrow of one of the fundamental results of the eddy viscosity and mixing length theories, was obtained when the shear stress profile was calculated from the observed mean velocity profile and chordwise development of the shear layer (Fig. 8). The constant of integration was determined from the measured wall shear stress. Although the behaviour of surface pitot tubes in a highly turbulent flow is not well known, the measured wall shear stress is likely to be too *high* rather than too low, and is most unlikely to be more than 10 per cent in error. It was found that the shear stress at the velocity peak was non-zero, being roughly *equal and opposite to the wall shear stress.* This was later confirmed to a fair accuracy by hot wire measurements, justifying the conclusion that the shear stress is definitely non-zero at the peak, contrary to any plausible hypothesis about eddy viscosity or mixing length and also to the results of Förthmann[5]. He calculated shear stress from the mean velocity profiles and assumed that the shear stress was zero at the outer edge of the layer, so it followed that the shear stress was also approximately zero at the velocity peak. Förthmann's mean velocity profiles, like the present ones, appear to fall to zero at the outer edge more quickly than expected (because of incidence effect on the pitot tube) and therefore his shear stress curve will be displaced vertically because of the error near the outer edge. Förthmann's shear profile shape otherwise agrees well with the present results. Förthmann's calculated wall stress appears to be about twice the value found by direct measurement and would lead to a ridiculous inner law. Liepmann and Laufer[19] also found errors near the outer edge in calculating shear stress across a

mixing layer: clearly calculations are not to be relied on in this region. It is most unfortunate that Förthmann's results of 1934 led him to the conclusion that the mixing length theory was valid in an asymmetrical jet.

The present calculations based on integration from a known wall shear stress give an excellent demonstration of the lack of dependence of the Reynolds stress on the mean velocity gradient: clearly both the mean and turbulent velocity profiles, which are basically of the free jet type, will be affected by the presence of the wall, but there is no *a priori* reason to suppose that there is a strong condition (other than the mean motion equation) connecting the influences on the two profiles in such a way as to ensure that the sign of the Reynolds stress always follows that of the mean velocity gradient. It is found in other flows that the two quantities are of the same sign, and what is the same thing that in the case of free jets and wakes the Reynolds stress is zero at the peak: of course this latter fact is deducible from symmetry alone, and presumably the reason why discrepancies have not been found previously is the concentration of effort on symmetrical free shear layers.* The only previous example of a flow with a Reynolds shear stress of opposite sign to the velocity gradient is the asymmetrical laminar jet instability problem discussed theoretically by Foote and Lin[20] but here the Reynolds stress correlation is confined to one wave-number and, to be fair, one should not attempt any comparison with the highly random quasi-molecular motion hypothesized by Prandtl. A minor point which should be mentioned is that the turbulent velocity near the peak is a very high percentage of the mean (much higher in fact that the percentage difference in velocity between the points where $\tau = 0$ and where $\partial u/\partial y = 0$), so that it it is at least *possible* that negative values of uv are always associated with positive values of instantaneous velocity gradient, but this would be a poor justification of the eddy viscosity idea and needless to say there is no evidence for any such association. It may be remarked here that there is no question of the experimental location of the velocity peak being seriously in error: the only reason for this would be the effects of mean velocity normal to the surface and of turbulent velocity gradient on the pitot tube and both these quantities are small.

General Accuracy of Glauert's Theory. Despite these two considerable discrepancies between theory and practice, of which the former, the discrepancy in wall layer velocity profile, is entirely due to the arbitrary choice of the pipe skin friction formula and power law and in no way a shortcoming of the method, Glauert's analysis succeeds in predicting accurately most of the features of the flow in a turbulent wall jet in still air, and its most important assumption, that of approximate Reynolds number similarity, is confirmed by the various sets of experimental results so far obtained.

Surface Friction in the Wall Jet. As mentioned, the surface tube measurements of the present experiment plot well on

$$\frac{\tau_0}{\frac{1}{2}\rho U_j^2} = 0{\cdot}0315 \left(\frac{U_j \delta_j}{\nu}\right)^{-0{\cdot}182}$$

in the region of $U_j\delta_j/\nu = 10^4$, and agree in this region with the results of Sigalla

$$\frac{\tau_0}{\frac{1}{2}\rho U_j^2} = 0{\cdot}0565 \left(\frac{U_j \delta_j}{\nu}\right)^{-0{\cdot}25}$$

obtained with Preston tubes. The agreement is largely fortuitous, since Sigalla assumed that Preston's pipe calibration[21] would also hold in a wall jet, whereas the present results show that the

* Tritton (Ph.D. Thesis, Cambridge University, 1959) found a negative eddy viscosity in a thermal convection wall jet over a heated inclined plate.

Preston tube calibration (Fig. 9) falls between those for the pipe and boundary layer[22]. Sigalla's values of $\tau_0 d^2/4\rho\nu^2 = (u_\tau r/\nu)^2$, the non-dimensional tube radius, seem to have been in the region of 10^3, where the value of shear stress obtained from the present calibration is about 6 per cent higher than that derived from the pipe calibration: this difference is almost within the scatter of Sigalla's results, and there is also some slight justification for fitting a smaller negative slope than 1/4, to the plotted points, which would then bring them more into line with the present results.

Streamwise Development. The best power law fits to the streamwise variation of peak velocity and layer thickness give exponents near $-0{\cdot}5$ and $1{\cdot}0$ respectively (Fig. 3). Values of exactly $-0{\cdot}5$ and $1{\cdot}0$ are obtained in the free jet so it is seen that the influence of the wall is fairly small, most of the streamwise variation being caused by entrainment of mass from the surrounding fluid by the jet layer rather than loss of momentum to the wall by the wall layer. It is to be noted that the chosen exponents of $a = -0{\cdot}53$, $b = 0{\cdot}91$ do not tally with the slope $-0{\cdot}182$ of the skin friction graph (for similar profiles one would expect the slope to be $(b-1)/(a+b)$ or $-0{\cdot}24$ approx.), but the accuracy of the exponents is not sufficient for this to be significant.

Flow near the Jet Orifice. No allowance has been made for any shift in the virtual origin of the power-law variations: Sigalla found that the origin of the velocity variation coincided with the orifice, and that the origin of the thickness variation was about eight slot heights behind the orifice for an arrangement in which the nozzle lip (in the present terminology) was about eleven slot heights and in which the exit velocity profile was practically uniform. The virtual origin will depend strongly on the nozzle exit velocity profile and the nature of the boundary near the nozzle (*i.e.*, on whether the jet flows along an infinite flat plate, a semi-infinite flat plate, or one of two semi-infinite perpendicular flat plates) which affects the entrainment in this region. In the case where the exit velocity profile is essentially uniform a boundary layer will form on the wall and a mixing layer at the lip. The free-mixing layer was investigated by Liepmann and Laufer[19] in 1947 in the same condition as the present experiment, but they did not publish any measurements in the subsequent fully-developed wall jet. They found that the mixing layer spread towards the wall at an angle of about $\tan^{-1} 0{\cdot}085$ and outwards into still air at $\tan^{-1} 0{\cdot}2$. The rate of spread of the boundary layer depends on Reynolds number, but it is clear that for nearly ten slot heights downstream a core of undiminished total pressure will exist and probably that for an even greater distance the wall jet will be incompletely developed. Sigalla, using a slot of height $0{\cdot}313$ in., made some measurements of the peak velocity, the rate of spread of the jet and the skin friction which all showed that full development was attained between ten and twenty slot heights downstream but he did not publish any velocity profiles in this region: his graph of the rate of spread of the free mixing layer agrees with Liepmann and Laufer's.

The Entrained Flow. The external potential flow due to the entrainment of fluid is roughly the same as the upper half of that due to a free jet in the same conditions. The streamlines in this case are confocal parabolae with the orifice as focus: the stream function is

$$\psi(r, \theta) = -2qr^{1/2} \frac{\cos \theta/2}{\cos \theta_0/2}$$

where the circumferential component of inflow velocity at the edge of the jet, $\theta = \theta_0$, is $qr^{-1/2}$: the inflow velocity into the *wall* jet, $\frac{d}{dx}\int_0^\delta U dy$, is approximately proportional to $r^{-0{\cdot}4}$ but the theoretical solution for this case would be much more complicated. The streamlines for the free jet are plotted

for equal intervals of ψ in Fig. 10. The velocity on the axis upstream of the nozzle is $2qr^{-1/2}/\cos(\theta_0/2) \simeq 2qr^{-1/2}$, that is, twice the vertical inflow velocity at the same distance downstream of the nozzle.

Turbulence Structure of the Wall Layer. The turbulent velocity profiles in the wall jet (Fig. 11) shown an extremely high value of $\tilde{u}/U$ near the wall, compared with the values found in a boundary layer by Klebanoff[23] and in a pipe by Laufer[18]. It is evident that most of the turbulent energy diffuses from the intense, larger-scale fluctuations in the jet layer, as the advection and production terms near the wall will be of the same order as in a boundary layer. One would therefore expect the excess energy to reside chiefly in the lower wave-numbers, and that the $R_{11}(o, r, o)$ correlation (streamwise velocity components at two vertically separated points) at say $y = \delta_j/4$ would have a 'tail' extending well out into the jet layer. This is certainly found in practice as seen by Fig. 12 in which a most pronounced double structure exists. The correlation curve can be divided quite well into two (uncorrelated) motions, one contributing 60 per cent of the whole and with an integral scale $0{\cdot}4\delta_j$, composed of eddies of a large range of sizes, representing wall-generated turbulence of about the same intensity as in a pipe or boundary layer, and the other of intensity 40 per cent of the whole, integral scale $1{\cdot}75\delta_j$, with a more restricted range of eddy sizes, representing that part of the turbulence which is diffused from the jet layer. We note that this latter motion is capable of convecting sheared fluid into the wall layer from distances of the order of $2\delta_j$ from the wall, that is from a region well inside the jet layer where the shear stress is undoubtedly of opposite sign to that at the wall. Therefore, packets of fluid having negative shear stress will frequently penetrate into the wall layer. This explains, in terms of the turbulence structure, the observed extension of the jet layer sign of shear stress into the wall layer.

Turbulence Structure of the Jet Layer. The turbulence in the outer part of the wall jet may be compared with that in the free mixing layer investigated by Liepmann and Laufer. In Fig. 13 the two sets of results are plotted against what seemed to be the best length scale, $(y-\delta_{0{\cdot}5})/\delta_f$, where $\delta_f = U_{\max}/(\partial U/\partial y)_{\delta_{0{\cdot}5}}$ is a length based on the slope of the mean velocity profile at the inflexion; it is seen that they are broadly similar though it would be more satisfactory to compare results for the two-dimensional wall jet with the two-dimensional free jet. It is interesting to notice that both the u and v components of turbulence in the wall jet are higher than in the mixing layer except near the outer edge where they coincide within the likely accuracy of the measurements (very poor in this region for reasons explained in Section 3). In particular, at $(y-\delta_{0{\cdot}5})/\delta_f = -0{\cdot}6$, which is the peak of the wall jet and near the high-velocity edge of the mixing layer, the u component is $5{\cdot}5$ per cent in the mixing layer and 21 per cent in the wall jet. It is unfortunate that no detailed measurements of turbulence in the two-dimensional jet are available. The only recent work seems to be that of v.d. Hegge Zijnen[24] who measured $\tilde{u}$, $\tilde{v}$ and uv with a constant-current anemometer in a low-speed jet. Measurements of correlation, like those made by Grant[25] in the wake and in the boundary layer, would be very useful. The two-dimensional jet turbulence (u-component only) measured at the N.P.L. seems to correspond more closely with the wall jet than the mixing layer does.

4.2. *Wall Jet in Still Air on Curved Surface (Coanda Effect).* The Coanda or 'teapot' effect of the continued attachment of a jet of fluid to a curved surface inserted into it has long been a subject of controversy. Attempts have been made to put forward a simple reason for this apparently unexpected phenomenon. The usual explanation of attachment of a fluid-into-fluid jet is that the solid surface obstructs entrainment of the surrounding fluid by the jet and the resulting, or incipient, suction force between jet and surface causes the jet to remain attached. This effect undoubtedly exists, and can be observed even in a circular jet a short distance above a *flat* surface, which is

attracted in much the manner described, but it is obvious that this cannot account for the attachment of a fluid-into-vacuum jet or, what is nearly the same thing, a water-into-air jet where entrainment is non-existent. Lighthill[26] has shown that a potential flow in which a jet is deflected round a curved surface does in fact exist: it is transformable into a semi-circular hodograph. In practice the flow will be modified by viscosity and the growth of a boundary layer on the surface will hasten separation, but it seems that the mysterious phenomenon is not the 'Coanda effect' itself but the disagreement of physical intuition with both mathematics and practice.

The possible configurations of jets and obstacles are infinite in number, but the study of the wall jet on a flat surface led naturally to experiments with a wall jet on a cylinder so that only separation, and not the circumstances of initial attachment, was investigated.

Increased Growth of Jet Thickness on Curved Surface. The immediately interesting part of the results is the discovery that the growth of the jet thickness on the cylinder was still almost linear but at roughly 1·5 times the rate of that on the flat plate, even where the jet was far from separation (Fig. 14). In fact it was found that as the jet momentum flux decreased only slowly with distance and the radius of curvature was constant, the pressure on the surface

$$p_a - p_0 = \int_0^\infty \frac{\rho U^2}{R}\, dy \doteq \frac{1}{R_0}\int_0^\infty \rho U^2 dy \text{ as } R_0 \gg \delta, \doteq \frac{\text{total jet momentum flux}}{\text{radius of cylinder}}$$

remained almost constant before rising rapidly in the region of changing streamline curvature just before separation (Fig. 15). The velocity profiles in fully attached flow (Fig. 16) were nearly the same as in the wall jet on a flat surface, and surface friction values are comparable, though it should be pointed out that the surface friction values shown were derived from the assumption that I_2 was the same as on the flat surface (Fig. 17). Nearer the separation point the wall layer grew relatively more quickly, the surface friction coefficient decreased, and the flow finally left the surface at about 150 deg round the cylinder from the slot. The separation point is likely to depend rather critically on the endplate size and the downstream geometry, both of which affect entrainment: there would be no separation at all in the inviscid case of a jet issuing from a slot in a cylinder.

The possible reasons for the increased initial growth of the jet are two. The more obvious is the effect of the entrained air which appeared to move spirally and intersect the jet at an acute angle to the surface in marked contrast to the flow external to the plane jet. The fictitious sink distribution in this case would be rather complicated and the mathematical solution for the potential flow correspondingly more difficult and less general, but Fig. 18 gives an idea of the general characteristics. However, one would expect the nearly circumferential inflow to retard, rather than advance, mixing.

Possibility of Centrifugal Instability. Another possible reason for the decreased mixing rate is the presence of an unstable gradient of angular momentum in the jet layer, in which $Ur(\doteq UR_0$ as $\delta/R \ll 1)$ decreases outwards. It is well known that this effect may produce streamwise vortices in both laminar and turbulent flow, which might reinforce the large eddy structure hypothesized by Townsend[27]. It is therefore to be expected that a tendency to the formation of such vortices would increase the shear parameter and the mixing rate. In addition, a large eddy crudely regarded as rotating as a solid body with angular velocity vector $\boldsymbol{\Omega}$ would experience a couple $-\boldsymbol{\Omega} \times \boldsymbol{\omega} I$ where $\boldsymbol{\omega}$ is the meanflow angular velocity vector and I is the moment of inertia in the $\boldsymbol{\omega}$ direction. If the moment of inertia in the $\boldsymbol{\Omega} \times \boldsymbol{\omega}$ direction is also I, the angular acceleration of the eddy will be $\boldsymbol{\Omega} \times \boldsymbol{\omega}$

$$|\boldsymbol{\omega}| \doteq \frac{U}{R} = 50 \text{ rad/sec, say, using values appropriate to the present tests.}$$

$$|\boldsymbol{\Omega}| = \frac{\tilde{u}}{r} = 3 \text{ rad/sec, say, (assuming the large eddy R.M.S. intensity to be 5 per cent}$$

of the whole turbulent intensity and therefore 1 per cent of the mean velocity. The radius will be of the order of half the jet layer width).

The life of a large eddy[27] is about $3/(\partial U/\partial y) \simeq 3/200$ sec, and thus the angular velocity acquired at the end of it will be about 2 rad/sec, which is of the same order as the initial angular velocity Ω in the perpendicular direction, so that the equilibrium large eddy structure in the wall jet on a curved surface might be quite different from that of the plane jet, and in particular one might expect the hypothesized tendency to longitudinal vortices to show up as an increased backflow and a large negative region in the R_{22} (o, o, r) correlation at, say $y = \delta_{0\cdot5}$. This correlation has been measured in the plane jet and on the cylinder (Fig. 19) but no such effect is visible. In view of the scatter in the results it is difficult to say whether or not there is a greater negative correlation on the cylinder than on the flat plate, but there are certainly no signs of an overpowering backflow, so either the vortices are on a quite different scale to the large eddies, or exist further out in the flow near the extreme edge of the jet where hot-wire measurements are dubious, or they do not exist, and the cause of the increased growth rate must be sought elsewhere.

If an element of fluid in the jet layer acquired an increase in velocity in the circumferential direction u, say, it would tend to accelerate in the radial direction at a rate $2Uu/R$. There would thus be a positive correlation uv, further augmented by the fact that the high-speed fluid element would enter a region of lower mean velocity. One would therefore expect a numerical increase in the shear stress in the outer part of the jet above the value for a plane wall jet by an amount inversely proportional to the radius of the cylinder, but an explanation would require measurement of all nine R_{ii} correlations in the free jet, the wall jet and the cylinder jet and it was not felt reasonable to attempt this with the hot-wire apparatus available at the moment.

The u-component turbulence in the cylinder jet (Fig. 20) is much the same as in the wall jet except near the outer edge where it is rather less, both as a percentage of the local mean velocity and of the peak velocity.

4.3. *Wall Jet Mixing with a Uniform External Stream.* We have seen that the outer part of the velocity profile of the wall jet on a curved surface differs from that on a flat surface because of differences in the inflow angle of the entrained fluid. The action of an external stream is far more noticeable, although the general behaviour of the shear layer is similar to the still-air case. Most of the practical interest in wall jets is in flows with an external stream and particularly in the mixing of a wall jet with a boundary layer in adverse pressure gradient.

Invalidity of Flow Constant in Jet Layer. The first arrangement to be studied experimentally was the mixing of a wall jet with a thin boundary layer, which was soon absorbed entirely thus allowing the jet to mix directly with the free stream. Here, the velocity difference across the jet layer is no longer equal to the peak velocity so that the profiles are not similar (Fig. 21), although both the wall layer and jet layer profiles are approximately similar among themselves when compared on suitable scales, such as U/U_j, y/δ_j for the wall layer (Fig. 22) and $(U_j - U)/(U_j - U_1)$, $(y - \delta_j)/\delta_f$ for the jet layer (Fig. 23). This leads one to think of an extension of Glauert's calculation method using an empirical surface friction formula and eddy viscosity and applying momentum considerations to each layer separately. A similar method based on mixing length theory has been developed by Stratford[28] for two-dimensional diffuser flow. Unfortunately we may again expect the shear stress at the peak to be non-zero and in addition the jet layer flow constant—such as it is—will not necessarily be genuinely the same for all values of U_j/U_1. Clearly, the flow constant for very large

velocity ratios ought to tend towards that for a still-air wall jet, whereas that for a ratio near to unity will be nearer that in a wake or the outer layer of a boundary layer. Ref. 8 collects various results for turbulent free jets in a moving stream and suggests a theory based on a constant value of $(U_j - U_1)\delta/\nu_\tau$ equal to that for the jet in still air. This theory becomes inaccurate if the free-stream velocity is more than about $0{\cdot}3U_j$. Carrière *et al*[10] constructed a formula for eddy viscosity which was intended to revert to the *free* jet form for $U_1 = 0$, but it does not appear to approach the wake form for small velocity ratios and in any case is intended for use in the sort of method we have just been forced to reject. Even in the case of a symmetrical jet in a free stream the use of a flow constant is dubious: if we define a flow constant as $R = (\Delta U)\delta_f/\nu_\tau$ (δ_f is the best thickness to use for comparing the slightly differing profiles of various types of free shear layer), the values are

$2-D$ Mixing Layer	48
$2-D$ Free Jet	48
$2-D$ Wall Jet	67
$2-D$ Cylinder Jet	47
$2-D$ Wake	23

Clearly a symmetrical jet discharging parallel to a uniform stream will gradually tend towards a wake (with negative velocity defect) so that the flow constant, initially 48, will finally become 23. In the intermediate region, where the velocity excess in the jet is of the same order as the free-stream velocity, it follows from the discussion on pp. 90 to 93 of Ref. 27 that the flow cannot be exactly self-preserving although the mean velocity profiles may appear accurately similar owing to the small difference between the profiles in the extreme case of jet and wake. Therefore, any 'flow constant' introduced is liable to depend on upstream conditions, as indeed is found in practice, although it may be useful for engineering calculation methods in a restricted range of flow. In the case of an accelerating free stream, the velocity profile is found to be distorted so that an eddy viscosity constant across the shear layer is not likely to describe the flow adequately and would in any case be a function of so many variables that its experimental determination would be difficult. The whole idea of large eddy equilibrium would break down if the static pressure altered considerably during the typical lifetime of such an eddy, which Townsend suggests is 'at least three time the reciprocal of the typical mean rate of strain' or about $3\delta_f/(U_j - U_l)$, the distance travelled being therefore $3\delta_f(U_j + U_l)/2(U_j - U_l)$ or about 4 in. in the case of the profile at 5·95 in. from the slot: this distance is not negligible compared with a typical value of $U_j/(dU_1/dx)$.

Difficulties of Calculating the Wall Jet Development. We therefore find that we must abandon the proposed calculation method because of the large number of inaccuracies from which it is likely to suffer. These are

(i) Effect of non-zero shear stress at velocity extrema.

(ii) Inadequacy of $c_f = f(R_{\delta_j})$ type of formula in strong adverse pressure gradient.

(iii) Probable lack of self-preservation of free shear layer intermediate between wake and jet.

(iv) Effect of pressure gradient on structure of free shear layers.

(ii), (iii) and (iv), of which (ii) is also a failing of existing boundary-layer calculation methods, would not be too serious, and were foreseen, but the addition of (i) makes one feel that a simple method of calculation would inevitably degenerate into a mere data correlation.

The experimental results for the wall jet mixing with a constant-velocity free stream (Fig. 21) show that the jet layer has a longer 'tail' than that observed in still air but, as mentioned before, this is attributable to the effect of pitot incidence in the latter case. The other features of the results are better discussed in connection with the case of wall jet mixing with a boundary layer, which has been analysed in greater detail.

4.4. *Wall Jet Mixing with a Boundary Layer.* In the arrangement tested, the initial boundary-layer momentum thickness was about one-fifth of the numerical value of the initial jet momentum thickness $\int_0^h \frac{U_{j0}}{U_1}\left(1-\frac{U_{j0}}{U_1}\right)dy$; this latter quantity was of course negative. It is seen from the results (Fig. 24) that the velocity at the trough, zero just downstream of the lip, rose to $0\cdot8U_1$ within a streamwise distance of one inch or half a boundary-layer thickness, at which point U_j/U_1, initially $5\cdot5$, was still as high as $2\cdot5$: in other words the greater part of the boundary-layer velocity defect is absorbed so quickly that the jet layer velocity difference is effectively $U_j - U_1$. This does not hold further downstream, as dU_t/dx decreases quickly, partly because $\partial U/\partial y$ decreases in the outer part of the boundary layer and partly because $d\delta_t/dx$ decreases downstream, a reflection of the transition from a jet-type ($\delta \propto x$) to a wake-type ($\delta \propto x^{1/2}$) free shear layer. In fact $(U_j-U_t)/(U_j-U_1)$ the ratio of the jet layer velocity difference to the peak supervelocity, changes from its minimum value of $1\cdot14$ to $1\cdot6$ as x changes from 1 in. to 22 in., indicating that the peak would finally disappear before absorbing all the boundary layer whereas the same ratio in the case of mixing with a much thinner initial boundary layer tends rapidly to unity. At some intervening boundary-layer thickness the ratio would remain at a roughly constant value until peak and trough disappeared simultaneously.

The transition of $d\delta_t/dx$ from jet-type to wake-type growth shows that a wall jet necessarily mixes less quickly with a moving stream than with still air: only when U_j/U_t is very high will the growth rate approach that of the still-air wall jet, so that the latter value of $d\delta_t/dx$, $0\cdot125$, sets an outer limit to the region whose total pressure can be increased by tangential blowing, although the outer streamlines are of course displaced towards the surface by entrainment into the jet. This point will be mentioned again in the discussion of separation in adverse pressure gradient. We note that $d\delta_j/dx$ is roughly constant and equal to its value on a flat surface in still air, in other words the rate of growth of the wall layer is approximately independent of the peak velocity, just as $d\delta/dx$ for a turbulent boundary layer changes only slowly with Reynolds number. Unfortunately we shall see that this principle fails in adverse pressure gradient as it did in the case of the flow over a cylinder. Despite the relatively greater importance of the boundary layer velocity defect at some distance downstream of the slot, the jet peak velocities in the boundary-layer mixing and free-stream mixing cases are almost identical, at given x, up to the point where $U_j/U_1 \approx 1\cdot1$. Comparing the peak velocity with that in the still air case, we find that divergence occurs at about $U_j/U_1 = 2\cdot5$, so that there is clearly a limit to the extent to which one may assume the wall jet peak velocity to be independent of the trough velocity. It would have been more interesting to conduct experiments with a boundary layer having a more nearly linear velocity profile, perhaps produced by a non-homogeneous or yawed screen as used by Owen and Zienkiewicz[29], and Elder[30], as a wider range of profile could have been obtained.

The study of the mixing process was not carried as far as the point where the jet peak disappeared: it was still pronounced at the trailing edge 30 in. from the slot. A series of profiles was however taken at constant x and U_{j0} and varying U_1, in connection with surface friction measurements (Fig. 26)

and these show the gradual disappearance of the peak with decreasing $U_{j\,0}/U_1$. However the profiles with $U_j/U_1 < 1$ are not of much practical interest as in a flow with adverse pressure gradient this would indicate incipient separation. The variation of U_j/U_1 with $U_{j\,0}/U_1$ for this series of tests shows a rapid rise compared with the asymptotic rate of change where $U_{j\,0} \gg U_1$. By coincidence, the graph of U_j/U_1 against $\theta_{j\,0}/\theta_0$ is apparently a straight line, but this also conflicts with the asymptotic behaviour $U_j/U_1 \propto \sqrt{(\theta_{j\,0}/\theta_0)}$. δ_j decreases slightly as U_j/U_1 increases, tending to the 'still air' value of about 0·16 in., providing that U_j/U_1 is more than 1·2.

The profile parameter H_j has almost the same value for each profile of the variable jet velocity series, with a slight tendency for H_j to decrease as U_j/U_1 increases, approaching the 'still air' value $H_j \simeq 1{\cdot}28$. We note that the value of $\theta_{j\,0}/\theta_0$ at which peak and trough disappear simultaneously is likely to be about 4·5, much the same as in the main series of tests on boundary layer mixing.

Finite Shear Stress at Velocity Peak. The shear stress distribution was calculated from the measured mean velocity profiles for the boundary layer mixing case at $x = 8{\cdot}1$ in. (Fig. 27). The shear stress at the peak is about $-0{\cdot}27\tau_0$, whereas in the still air case it was about $-\tau_0$. This is understandable as $(U_j - U_l)/U_j$ is 0·24 as against unity in the latter case so that the effects of the jet layer on the wall layer may be expected to be proportionately less. The peak (negative) shear stress again corresponds almost exactly with the point of inflexion in the velocity profile. It was remarked by Liepmann and Laufer that there appears to be physical justification for this. Indeed, it is a consequence of assuming constant eddy viscosity across the flow, and is probably a feature of all equilibrium flows. One would not necessarily expect to find the same in a non-equilibrium flow like the present one and it may be merely a reflection of the fact that both the mean velocity gradient and the shear stress happen to take maximum values near the middle of the shear layer, so that a constant eddy viscosity of sorts can be defined for the central region of the flow, where the effects of the wall layer and the outer boundary layer (if any) are small.

A calculation of the eddy viscosity in the region of the point of inflexion shows that the local flow constant $R_T = (U_j - U_l)\delta_j/\nu_T$ is only 17 whereas the wake value is 23. Evidently the flow is far from self-preservation and the sheared fluid from upstream strongly affects the local conditions.

Shear Stress at the Velocity Minimum. A peculiarity is that the calculated shear stress reverses sign again *inside* the minimum velocity position. This might be taken as an indication that the outer boundary layer retained sufficient of its Reynolds shear stress to overpower the contrary shear stress in the jet layer. However, the outer boundary layer no longer receives any turbulent energy by diffusion from the wall, so that its only source of energy other than diffusion from the jet layer will be production proportional to the product of the Reynolds shear stress and the mean velocity gradient: we may therefore expect the Reynolds shear stress to decrease exponentially. Even the initial shear stress (of the boundary layer at the slot) is only about one-half of that required to oppose the jet layer shear stress, so we must suppose that the calculations of shear stress are in error at the trough as they are at the outer edge of the jet layer in still air. (The shear stress is obtained as $\tau_0 - \rho \int_0^y \left(U \frac{\partial U}{\partial x} + V \frac{\partial U}{\partial y} \right) dy$ so that errors may be expected to accumulate with increasing distance from the wall.) It is probable that the outer boundary layer may be treated as essentially inviscid, as suggested by Stratford in his method of calculating boundary-layer separation. The flow in the wall jet in the strong pressure gradient to be expected on a blown flap also satisfies the condition that the loss of kinetic energy in the outer layer due to pressure gradient should greatly exceed the loss due to turbulent dissipation.

Inner Law Velocity Profiles. The wall layer velocity profiles plotted as U/u_τ versus $u_\tau y/\nu$ show a pronounced semi-logarithmic region, unlike the profiles in the still air wall jet (Fig. 28). This is most interesting, because as mentioned in the discussion on the latter, one only expects a semi-logarithmic law when there is a simple defect law $(U_1 - U)/u_\tau = f(y/\delta_0)$. Now the existence of a defect law in the still air wall jet, which is to be expected on Glauert's hypothesis, was not very well confirmed by the experimental results, but the errors were not sufficiently large for it to be ruled out. We therefore decided that the defect law possibly existed but the semi-logarithmic overlap law definitely did not. In the case of the wall jet mixing with an external stream, Glauert's hypothesis is quite invalid, the outer layer scale varies in a different manner from the inner scale, and a defect law is even less likely. This is certainly borne out by the experimental results (Fig. 29) which show considerable deviation from a defect law although there is a true wall law which does not appear to vary with U_j/U_t in the region of interest, though it will of course revert to the still-air case wall law near the slot. Fortunately both profiles have an intercept $U/u_\tau = 16$ at $u_\tau y/\nu = 100$, and the skin friction values have been obtained on the assumption that this also holds for intervening values of U_j/U_t.

On the usual analysis, one would not expect a semi-logarithmic region, but in fact it does exist in the same range of Reynolds number as in the still air wall jet tests. This appearance of the semi-logarithmic law where it is not expected, following its absence where it *was* expected somewhat reduces one's confidence in the analysis which predicts it. One feels more inclined to say that the semi-logarithmic law appears in the wall jet with an external stream because the U/u_τ vs. $\log u_\tau y/\nu$ profile merely happens to have a point of inflexion like the boundary-layer profile, whereas the still air wall jet profile does not.

4.5. *Wall Jet Mixing with a Boundary Layer in an Adverse Pressure Gradient.* All the measurements reported in this case were made on the aerofoil with a 25 per cent chord flap deflected 46 deg and with the 0·040 in. slot. The 25 per cent L.E. flap was deflected about 9 deg sufficient to preserve attached flow over the upper surface. The jet slot velocity was chosen so as to give a firmly attached flow with a surface friction coefficient near the trailing edge of about 0·0012 based on velocity just outside the boundary layer (Fig. 30) compared with the zero pressure gradient value of about 0·003 at the same R_θ. The jet peak velocity near the trailing edge fell to $0{\cdot}8U_1$ (Fig. 37) so that a small decrease in jet exit velocity would cause the peak to disappear completely. It can be seen from Bernoulli's equation (considering inviscid flow) that the effect of adverse pressure gradient is to increase U_j/U_1 if this ratio is greater than unity but that when U_j/U_1 is less than unity viscous and pressure forces both tend to reduce it still further. The ratio does indeed fall more rapidly near the trailing edge. This shows the reason for the usual rapid rearward movement of separation point with increasing jet exit momentum implied by the steep gradient of the curve of C_L vs. C_μ found by other experimenters.

Flow near the Flap Knee: Effect of Surface Curvature. The flow near the flap knee is complicated by the large transverse pressure gradients which are a result of the surface curvature. Locally the (inviscid) flow approximates to that around an obtuse corner of angle 135 deg so that the static pressure gradient along any radius from the corner is proportional to $r^{-7/5}$. The velocity profiles (Figs. 32, 33, 34) near the knee are therefore strange-looking though the total pressure profiles (Fig. 35) are more familiar and it is probably justifiable to assume that since the region of severe transverse pressure gradient only extends chordwise for about three or four boundary-layer

thicknesses it has little effect on the total pressure profile of the outer boundary layer of the wall jet: the effect on the turbulence may be more marked but the assumption that the outer boundary layer can be treated as essentially inviscid is probably still justifiable.

We see that there is a large region of total pressure deficit just behind the blowing tube lip, which however disappears before the next traverse position 0·31 in. behind the slot. Assuming that the wall jet edge moves outwards at $\tan^{-1} 0{\cdot}12$ and that the aerofoil boundary-layer edge moves inwards at the same angle (a conservative estimate in view of the strong entrainment into the wall jet) the trough velocity would remain zero for about 0·2 in. behind the slot and then rise rapidly. The base pressure coefficient (with respect to static and dynamic pressure at infinity) is $-8{\cdot}64$ giving an increment in sectional drag coefficient of $+8{\cdot}64\ h/c = 0{\cdot}012$. The more serious effect is in the reduction of the total pressure increment due to the jet. The usual definition of momentum deficit thickness does not include stagnant layers because these produce identical increments in the momentum flux thickness $\int_0^\delta \left[1 - \left(\frac{U}{U_1}\right)^2\right] dy$ and the displacement thickness. In this case, however, we are interested in the momentum flux through the step in the surface, height $h + l$, so that the extra momentum available for boundary-layer control (compared with the momentum flux over an aerofoil without a step) is $\rho U_{j\,0}{}^2 h - \rho U_1{}^2(h+l)$. Actually the effect of the lip is smaller than would be expected if $\rho U_1{}^2(h+l)/h$ were subtracted from the jet momentum. Williams and Alexander[12] found that a lip thickness some 14 times the slot width roughly halved the effective value of $\rho U_{j\,0}{}^2 h$ in a region where $U_{j\,0}/U_1 \doteq 3{\cdot}3$ whereas the simple analysis would suggest that the effective value was negative. A general analysis of the flow near the slot in zero pressure gradient would be useful.

The effect of transverse pressure gradient on the wall jet is, fortunately, independent of the aerofoil pressure distribution and depends only on the local surface curvature. If $U_j/U_l \gg 1$ the flow will clearly be similar to that over a circular cylinder in still air, further complicated by the longitudinal pressure gradient. The value of $\delta_{0{\cdot}5}/R_0$ near the slot in the present case was of the order of 1/10 ,which is the same as that in the circular cylinder case at $x = 8{\cdot}51$ in. where the jet was still firmly attached and the profiles nearly similar to those on the flat surface with about 1·7 times the thickness. With a slot height of 0·040 in., the jet would not become fully developed for a distance of about $15h$ or 0·6 in. which is nearly the extent of the curved surface, so that it is probable that the effects of incomplete development and longitudinal pressure gradient are more important than that of surface curvature. It should be noted however that the direct effect of surface curvature is a favourable one in that it produces an increase in the rate of entrainment.

Variation of Peak Velocity. Secondary effects of surface curvature are seen in the very rapid increase in δ_j and δ_t and the correspondingly rapid fall in U_j between $x = 0{\cdot}87$ in. and $x = 2{\cdot}18$ in. which are caused by the sudden increase in surface radius of curvature and disappearance of normal pressure gradient in this region. The adverse pressure gradient at the surface is much larger than that at the edge of the boundary layer so that retardation of the fluid is also greater. The pressure difference across the shear layer is increased by the presence of the high velocity jet: this accounts for part of the sudden fall in surface pressure at the slot.

The value of $U_{j\,0}/U_1$ is about 2·03, where U_1 here denotes the velocity at the edge of the boundary layer. U_j/U_1 falls rapidly to 1·1 two inches from the slot (Fig. 36) and thereafter decreases quite slowly, although of course U_j and U_1 continue to decrease rapidly. The flow over the central regions of the flap may therefore not be too far from equilibrium and profile similarity: moreover

the conditions found in the present experiment are fairly typical of those on an aircraft blown flap where, in order to reduce the risk of separation, it is necessary to have $(U_j/U_1)_{TE} \geqslant 1$, so that some discussion of the implication of near-equilibrium may be useful.

Variation of Equilibrium Parameter. It was observed that the free-stream velocity over the central region of the flap (Fig. 37) was proportional to $x^{-1/2}$ approx. If the behaviour of an equilibrium wall jet is anything like that of a boundary layer which eventually separates if the free-stream velocity decreases more rapidly than about $x^{-1/3}$, then the flow cannot be in exact equilibrium and the equilibrium parameter $(\theta_j/\tau_0)(dp/dx)$ will increase with x. Using surface friction values obtained from the postulate that $U/u_\tau = 16$ at $u_\tau y/\nu = 100$, as in zero pressure gradient (which as seen in Fig. 38 gives reasonable results for the inner profile except for the region of pitot displacement error near the wall) we see (Fig. 30) that $(\theta_j/\tau_0)(dp/dx)$ actually decreases over the front section of the flap, is almost constant in the middle, and rises again towards the trailing edge. The profile parameter H_j behaves similarly though it is a less sensitive indicator and the values are more scattered. It does not seem likely that the decrease in H_j is attributable entirely to the increase in $R\delta_j$ as the values of H_j are all much larger than those in zero pressure gradient, indicating that the adverse pressure gradient must be largely responsible: this is borne out by the correlation between H_j and $(\theta_j/\tau_0)/(dp/dx)$ (Fig. 31) which is similar to that suggested by Clauser[31] for the equilibrium turbulent boundary layer except for the first two or three points. The aforementioned effects of rapid change of surface curvature may also extend to an influence on H. The surface friction coefficient $c_f = \tau_0/\frac{1}{2}\rho U_j^2$ falls monotonically with increasing x. The behaviour of $(\theta_j/\tau_0)/(dp/dx)$ leads one to believe that the wall jet is in some danger of separation near the knee, where although θ_j is small and τ_0 high, the adverse pressure gradient is very strong.

Modes of Separation. There are several possible modes of separation from a blown flap, depending on the pressure gradient and the initial boundary layer. They are

(i) reversed flow near the surface

(a) near the knee
(b) near the T.E.
} 'wall jet separation'

(ii) reversed flow at the velocity minimum

(a) almost certainly downstream of the knee alone—'boundary-layer separation'.

Obviously a trailing edge separation is preferable for reasons of safety. If a type (ii) separation occurred the jet would remain attached to the surface with a region of separated flow above it, and reattachment could only be ensured by blowing sufficiently hard for the boundary layer to be re-energized by entrainment of the fluid towards the surface (as in the still-air wall jet) rather than by direct mixing. The solution to the difficulty would be to move the jet slot forward of the minimum pressure point to ensure early mixing so that the trough velocity remained positive. A type (i) (a) separation would be almost independent of boundary-layer thickness and would only occur if the jet slot velocity were too low. A similar momentum flux from a narrow, high velocity jet slot would change the separation to type (i) (b).

No serious attempt was made to explore the flow in a separating wall jet. An excuse which might be put forward is that our chief interest in separation is directed towards suppressing it, but a more genuine reason is the doubt whether any really useful results would be obtained. Turbulent separation is such a complicated phenomenon that it should be studied in the simplest possible circumstances: the experimental complication of the wall jet flow, in which it is strictly necessary

to keep the external stream Reynolds number, the jet exit Reynolds number *and* the momentum coefficient constant from day to day, is excessive.

Turbulence Measurements. The results of the experiment on the deflected flap would have been more useful if extensive hot wire turbulence measurements could have been made. The shear stress distribution was not measured and the streamwise gradients are rather too large for successful calculation, but the distribution is likely to be much the same as in zero pressure gradient except that the maximum shear stress point will, as usual, move outwards from the wall so that τ_j/τ_0 may be numerically smaller, or even positive. The u-component of turbulence was measured at 3·97 in. aft of the nozzle and corresponds roughly to the still-air profile except that $\tilde{u}/U_j$ is smaller: a better correlation is obtained by remembering that the turbulence is largely generated in the jet layer and plotting $\tilde{u}/(U_j - U_l)$ for each case.

4.6. *General Discussion. Wall Jet in Still Air.* The results of the investigation of the wall jet in still air are satisfactory and seem to have clarified the behaviour of the flow. The conclusion of the inadequacy of the eddy viscosity hypothesis used by Glauert and by Carrière *et al.*, has largely frustrated the original purpose of developing a multi-layer calculation method for the blown flap, but as an exposure of the lack of rigour of the eddy viscosity concept it comes rather too late in the history of the subject. It is generally agreed that the choice of an eddy viscosity will permit quite accurate calculation of mean velocity profiles in simple cases such as the free jet and wake, but it is more properly regarded as a means of introducing an empirical constant than as a physically meaningful concept.

Coanda Effect. The investigation of the Coanda effect has demonstrated that the previously observed increased growth rate is caused, not by nearness to separation in adverse longitudinal pressure gradient, but probably by the negative radial gradient of angular momentum and resulting centrifugal instability of the turbulent flow.

Wall Jet below a Uniform Stream. The experiments on the wall jet below an external stream in zero pressure gradient show that the jet is not much affected by the boundary layer above it for values of $|\theta_{j0}/\theta_0|$ of the order of 5, which appears to be about the value at which the peak and trough disappear simultaneously. Presumably the behaviour of a wall jet mixing with a boundary layer in zero pressure gradient depends chiefly on θ_{j0}/θ_0, except near the slot where the ratio U_j/U_1 is the controlling parameter: except for the loss of momentum due to surface friction ($\Delta\theta_j = \frac{1}{2}\int c_f dx \doteq$ constant over a small range of Reynolds number) the flow is at constant momentum so that at least the gross characteristics of the flow will depend only on this momentum: a similar argument may be used to justify the use of C_μ as a parameter. We deduce the general result that in order for the tangential jet just to absorb the initial boundary layer the jet momentum excess must be about five times the boundary-layer momentum deficit.

Wall Jet below a Retarded Stream. This result cannot be extended to the case of a positive pressure gradient. $|\theta_{j0}/\theta_0|$ for the 46 deg deflected flap was little more than 2, although the transverse pressure gradients invalidate a simple calculation of this ratio: we have taken θ_0 as one-tenth the total thickness of the initial boundary layer. This value of $|\theta_{j0}/\theta_0|$ is sufficient to prevent separation but not enough to absorb the initial boundary layer altogether: clearly the flow will depend on the details of the aerofoil pressure gradient and one can only remark that absorption will probably occur at a lower value of $|\theta_{j0}/\theta_0|$ than in zero pressure gradient because of the relatively smaller retardation of the high-speed jet compared with the free stream and because of the smaller

surface friction coefficient. It seems improbable that a well-founded calculation method can be developed at the moment.

5. *Conclusions.* (1) The assumption made by previous workers that turbulent wall jet flow may be divided, for the purposes of calculation, into layers separated by the velocity extrema is invalid because the shear stress is non-zero at these points: this fact also demonstrates the physical unreality of hypotheses, such as those of mixing length and eddy viscosity, which postulate a simple connection between shear stress and mean velocity profiles.

(2) Despite (1), the theory due to Glauert[1] gives a good general description of the flow except that the Blasius pipe flow surface friction formula assumed by him underestimates the surface friction by about 25 per cent: a good data fit in the region $3000 < U_j\delta_j/\nu < 15{,}000$ is

$$\frac{\tau_0}{\frac{1}{2}\rho U_j^2} = 0{\cdot}0315\left(\frac{U_j\delta_j}{\nu}\right)^{-0{\cdot}182}$$

(3) Probably owing to the effects of centrifugal instability on the small-scale turbulence in the jet layer, the wall jet on a curved surface grows more quickly than that on a flat surface. The surface static pressure remains almost constant (for a given surface curvature) for flow sufficiently far from separation because of the approximate constancy of jet momentum flux.

(4) For the wall jet below an external stream in zero pressure gradient,

$$\frac{\tau_0}{\frac{1}{2}\rho U_j^2} \simeq 0{\cdot}026\left(\frac{U_j\delta_j}{\nu}\right)^{-0{\cdot}18}$$

for

$$\frac{U_j\delta_j}{\nu} \approx 10^4 \text{ and } 1 < \frac{U_j}{U_t} < 2.$$

The ratio of initial jet momentum thickness to initial boundary-layer momentum deficit thickness required for the jet just to absorb the boundary layer before the peak disappears is a little less than 5.

(5) In the case of the wall jet in still air, a fairly accurate outer law can be distinguished in the outer part of the wall layer: however the inner law is not semi-logarithmic. On the other hand, an outer law does not appear to exist for the wall jet below an external stream: but the inner law is quite accurately semi-logarithmic. This casts some doubt on the usual derivation of the semi-logarithmic overlap law.

(6) The wall jet below a retarded stream proves not to be amenable to calculation. It is found that separation from the surface is likely to follow soon after the ratio of the jet peak velocity to the free-stream velocity falls below unity (trailing-edge type separation) but it also appears that the wall jet may separate near the knee of the flap soon after the commencement of the adverse velocity gradient as the shape parameter H_j and the equilibrium parameter $(\theta_j/\tau_0)/(dp/dx)$ may take high values in this region. No simple laws suffice to describe the behaviour of the jet peak velocity and height as in the still air case. A worthwhile calculation method is unlikely to be developed without further knowledge of the processes of generation of turbulent shear stress.

Acknowledgements. The authors wish to acknowledge the benefit of several discussions with Dr. J. Williams and Mr. A. J. Alexander, both formerly of the Aerodynamics Division, N.P.L. They are grateful to Dr. J. T. Stuart for drawing their attention to Ref. 20, and to Dr. D. L. Schultz for much advice and assistance in the hot wire measurements. The calculations were performed by Miss L. M. Esson, and Mr. D. H. Ferriss assisted in some of the experimental work.

NOTATION

(Infrequently occurring symbols are defined on use)

a Exponent in power law for streamwise variation of wall jet peak velocity $U_j \propto x^a$

b Exponent in power law for streamwise variation of wall jet thickness $\delta_{0\cdot5} \propto x^b$

c Chord of aerofoil in 'blown flap' configuration (Fig. 1a)

$c_f = \frac{\tau_0}{\frac{1}{2}\rho U_j^2}$ Local surface friction coefficient based on jet peak velocity

C_μ Jet momentum coefficient

d Preston tube diameter

$H = \delta^*/\theta$ Shape parameter

I_2 Value of u/u_τ at $\log \frac{u_\tau y}{\nu} = 2$

h Jet orifice slot height

l Jet orifice lip height

P Stagnation pressure

p Static pressure

$q = \frac{1}{2}\rho U^2$ Dynamic pressure in incompressible flow

R Radius (cylinder wall jet)

r Radius (Preston tube)

$R_{ii}(x, y, z)$ Correlation coefficient, with separation components x, y, z of i-component turbulent fluctuation ($i = 1, 2, 3 \equiv u, v, w$)

U, V, W Mean velocity components

u, v, w Instantaneous turbulent fluctuation components

$\tilde{u}, \tilde{v}, \tilde{w}$ R.M.S. turbulent fluctuation

ΔU Velocity difference across free shear layer

$u_\tau = \sqrt{(\tau_0/\rho)}$ Friction velocity—see also list of suffixes

x Streamwise distance from jet orifice, in.

y Normal distance from surface, in.

z Cross-stream distance, in.

δ Boundary-layer thickness, in.

$\delta_f = \Delta U \left(\frac{\partial U}{\partial y}\right)_f$ where f refers to point of inflexion in free shear layer velocity profile

$\delta^* = \int_0^\delta \left(1 - \frac{U}{U_1}\right) dy$, displacement thickness

see also list of suffixes

$\eta = y/\delta_{0\cdot5}$

$\theta = \int_0^\delta \frac{U}{U_1}\left(1 - \frac{U}{U_1}\right) dy$, momentum deficit thickness

$\mathcal{K} = \frac{\nu_T}{U_j \delta_{0\cdot5}}$, reciprocal of flow constant

ν Kinematic viscosity

ν_T Eddy kinematic viscosity

ρ Density

τ Shear stress

Suffixes

0 Surface or jet orifice

1 Edge of boundary layer

∞ Free stream

j Jet peak (or jet inner layer regarded as boundary layer)

t Jet trough

REFERENCES

No.	*Author*	*Title, etc.*
1	M. B. Glauert	The wall jet. *J. Fluid Mech.* Vol. 1. p. 625. 1956.
2	P. Bakke	An experimental investigation of a wall jet. *J. Fluid Mech.* Vol. 2. p. 467. 1957.
3	A. Sigalla	Experimental data on turbulent wall jets. *Aircraft Engineering*. May, 1958. p. 131.
4	A. Sigalla	Measurements of skin friction in a plane turbulent wall jet. *J. R. Ae. Soc.* Vol. 62. p. 873. 1958.
5	E. Förthmann	Turbulent jet expansions. Translated as N.A.C.A. Tech. Memo. 789. 1936.
6	N. Tetervin	Laminar flow of a slightly viscous incompressible fluid that issues from a slit and passes over a flat plate. N.A.C.A. Tech. Note 1644. 1948.
7	H. B. Squire and J. Trouncer ..	Round jets in a general stream. A.R.C. R. & M. 1974. January, 1944.
8	G. N. Abramovich	The turbulent jet in a moving fluid. Unpublished M.O.A. Report.
9	M. F. Gates	Static lift characteristics of jet slots—a clarifying study of the external ejector. Hiller Aircraft Corp. Rep. ARD–213. Contract Nonr. 2428(00). 1958. p. 79942.
10	P. Carrière, E. A. Eichelbrenner and Ph. Poisson-Quinton.	Contribution théorique et experimentale à l'étude du contrôle de couche limite par soufflage. O.N.E.R.A. Rapport 1/2261A. 1958. Read at 2nd Int. Cong. Aero. Sci., Madrid.
11	S. F. J. Butler and J. Williams ..	Further comments on high-lift testing in wind tunnels with particular reference to jet blowing models. *Aero. Quart.* August, 1960. p. 285.
12	J. Williams and A. Alexander ..	Pressure-plotting measurements on an 8 per cent thick aerofoil with trailing-edge flap blowing. A.R.C. R. & M. 3087. June, 1956.
13	P. Bradshaw and N. Gregory ..	The determination of local turbulent skin friction from observations in the viscous sub-layer. A.R.C. R. & M. 3202. March, 1959.
14	S. Goldstein	*Modern Development in Fluid Dynamics*. p. 253. 1938.
15	R. Westley	Frequency response of pitot probes. N.A.E. (Canada). LR–214. 1957. p. 70259.
16	N. H. Johannesen	Further results on the mixing of free axially symmetrical jets of Mach number 1·40. A.R.C. 20,981. May, 1959.

REFERENCES—*continued*

No.	*Author*	*Title, etc.*
17	H. C. Garner and D. E. Walshe ..	Usefulness of various pressure probes in fluctuating low-speed flow. A.R.C. 21,714. February, 1960.
18	J. Laufer	The structure of turbulence in fully-developed pipe flow. N.A.C.A. Report 1174. 1954.
19	H. W. Liepmann and J. Laufer ..	Investigation of free turbulent mixing. N.A.C.A. Tech. Note 1257. August, 1947.
20	J. R. Foote and C. C. Lin	Some recent investigation in the theory of hydrodynamic stability. *Quart. App. Math.* Vol. 8. p. 265. 1950.
21	J. H. Preston	The determination of turbulent skin friction by means of pitot tubes. *J. R. Ae. Soc.* Vol. 58. p. 109. 1954.
22	Staff of Aerodynamics Division, N.P.L.	On the measurement of local surface friction on a flat plate by means of Preston tubes. A.R.C. R. & M. 3185. May, 1958.
23	P. S. Klebanoff	Characteristics of turbulence in a boundary layer with zero pressure gradient. N.A.C.A. Report 1247. 1955.
24	B. v. d. Hegge Zijnen	Turbulence measurements in a two-dimensional jet. *App. Sci. Res.* (A). Vol. 7. No. 4. p. 256. 1957.
25	H. L. Grant	The large eddies of turbulent motion. *J. Fluid Mech.* Vol. 4. Pt. II. pp. 149 to 190. 1958.
26	M. J. Lighthill	Notes on the deflection of jets by the insertion of curved surfaces and on the design of bends in wind tunnels. A.R.C. R. & M. 2105. September, 1945.
27	A. A. Townsend	*The structure of turbulent shear flow.* Cambridge University Press. 1956.
28	B. S. Stratford	Turbulent diffuser flow. A.R.C. C.P. 307. March, 1956.
29	P. R. Owen and H. K. Zienkiewicz..	The production of uniform shear flow in a wind tunnel. *J. Fluid Mech.* Vol. 2. Pt. VI. pp. 521 to 531. 1957.
30	J. W. Elder	Steady flow through non-uniform gauzes of arbitrary shape. *J. Fluid Mech.* Vol. 5. Pt. III. pp. 355 to 368. 1959.
31	F. H. Clauser	Turbulent boundary layer in adverse pressure gradients. *J. Ae. Sci.* Vol. 21. p. 91. 1954.

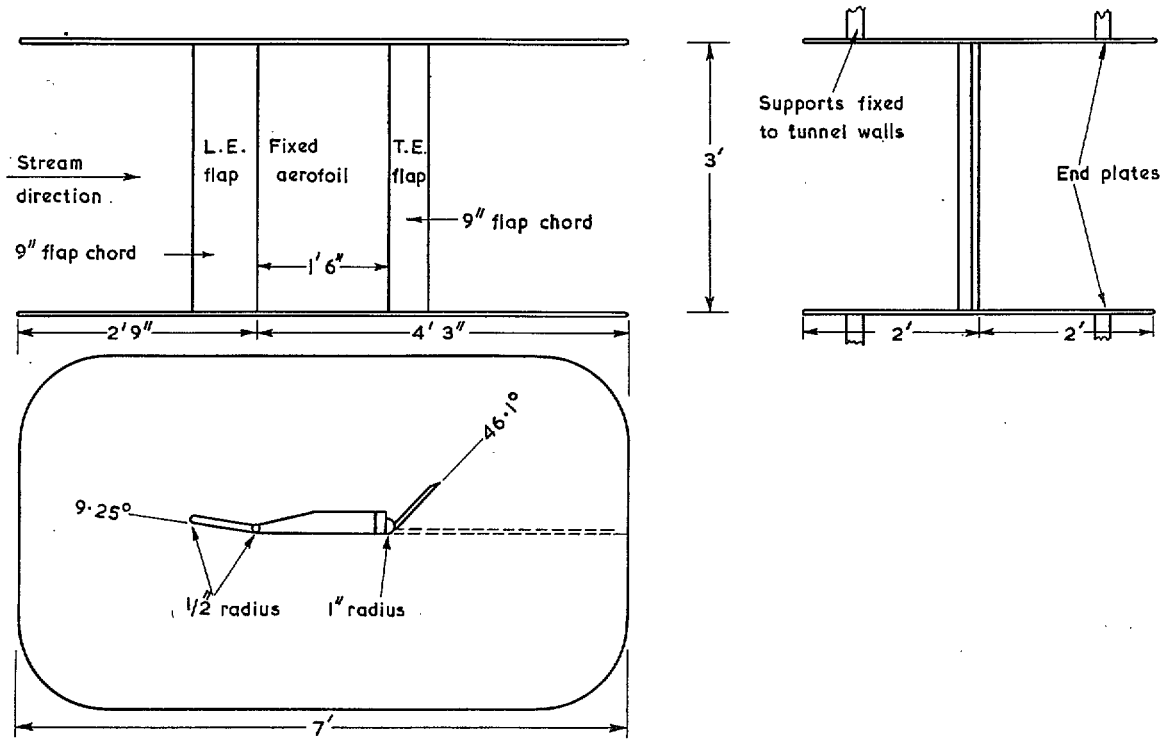

FIG. 1a. Apparatus—Test aerofoil mounted in N.P.L. 9′ × 7′ No. 2 Tunnel with plane of aerofoil vertical.

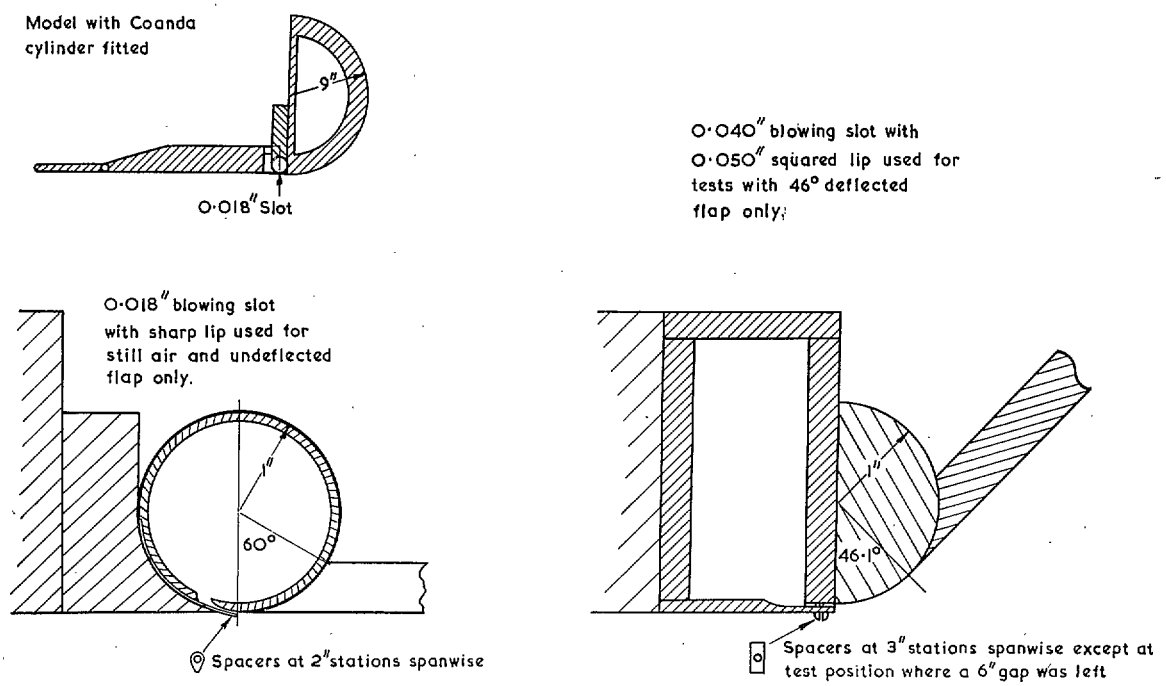

FIG. 1b. Blowing slots and Coanda cylinder.

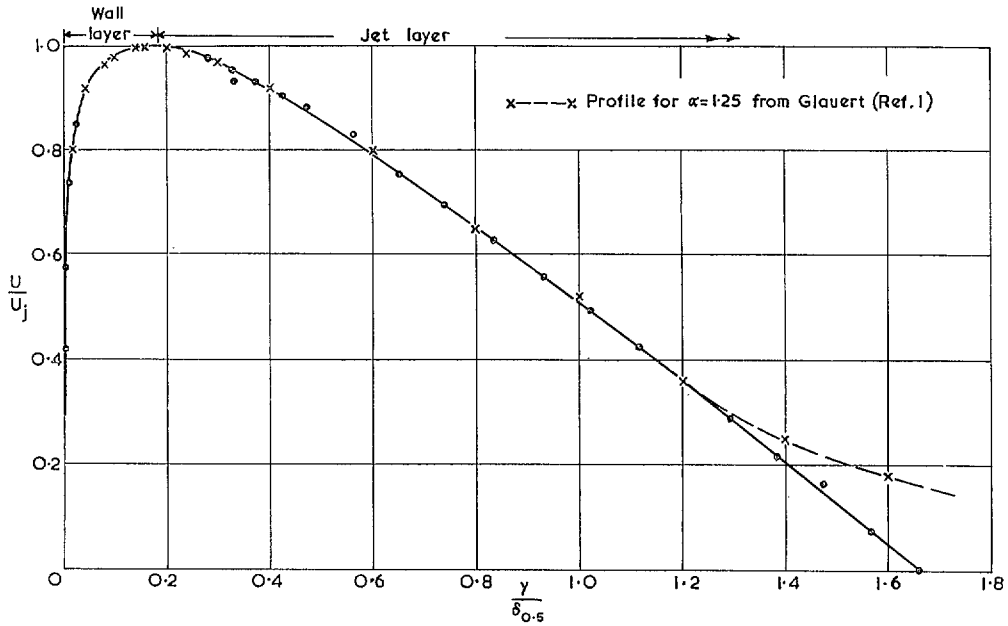

FIG. 2. Typical mean velocity profile—wall jet in still air on flat surface.

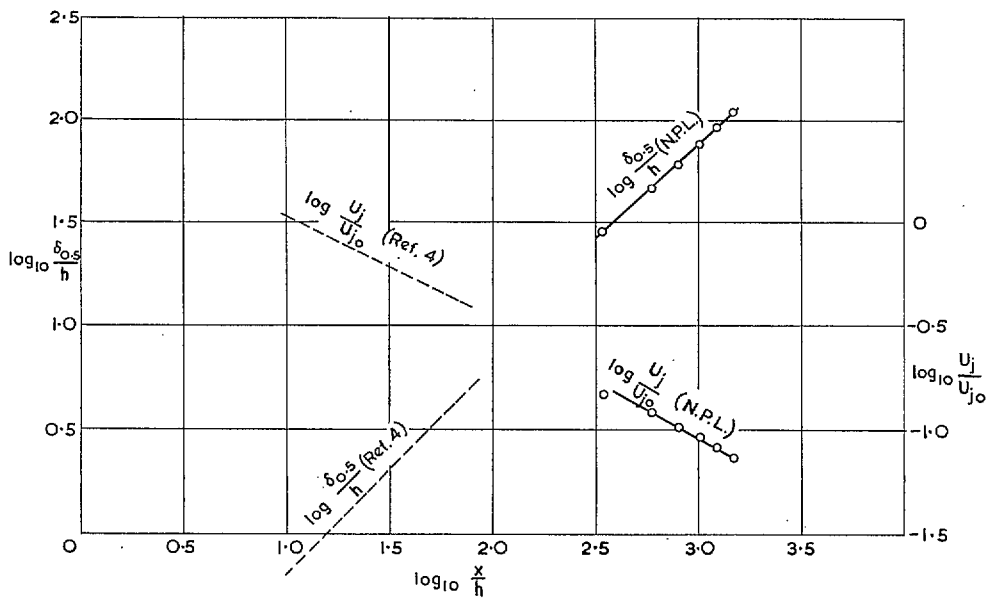

FIG. 3. Peak velocity and layer thickness variation—wall jet in still air on flat surface (*see* also Fig. 14).

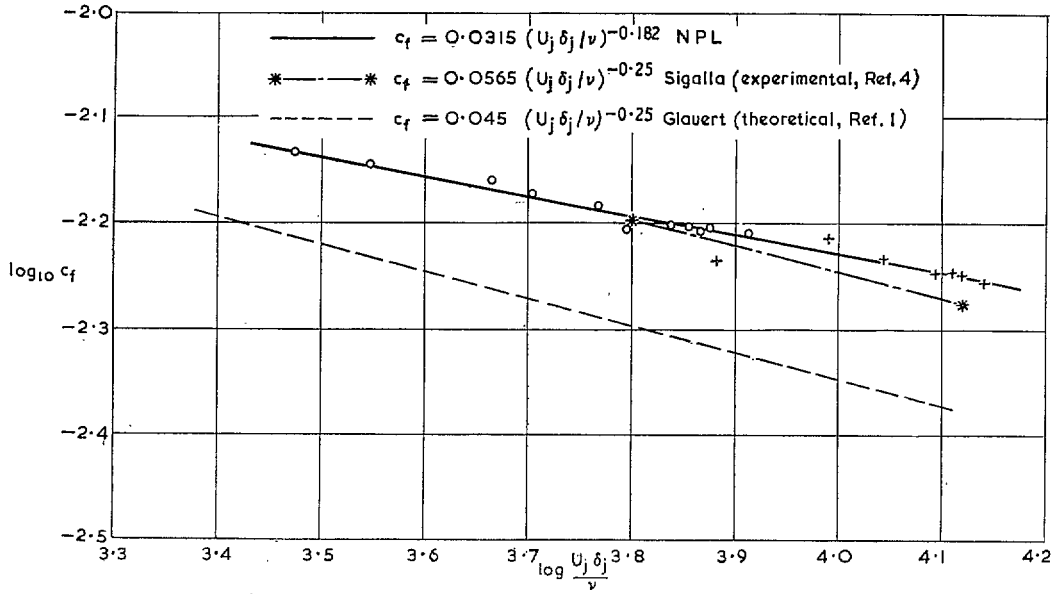

FIG. 4. Surface friction measurements—wall jet in still air on flat surface.

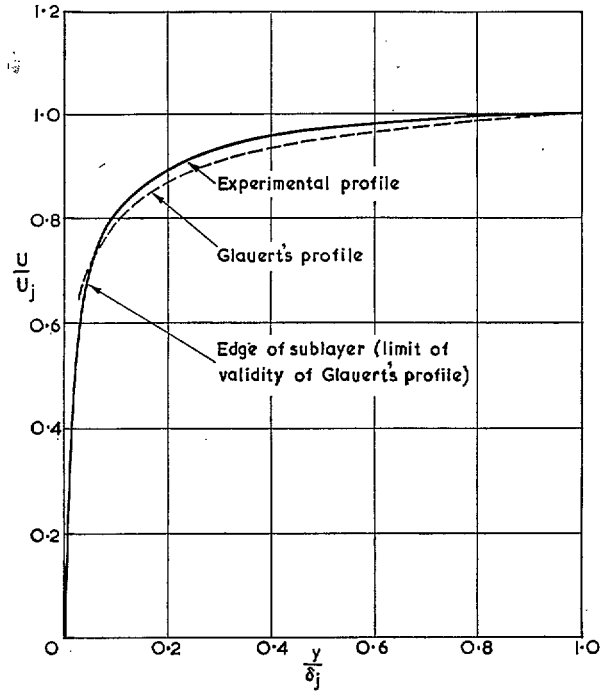

FIG. 5. Wall layer mean velocity profile—wall jet in still air on flat surface.

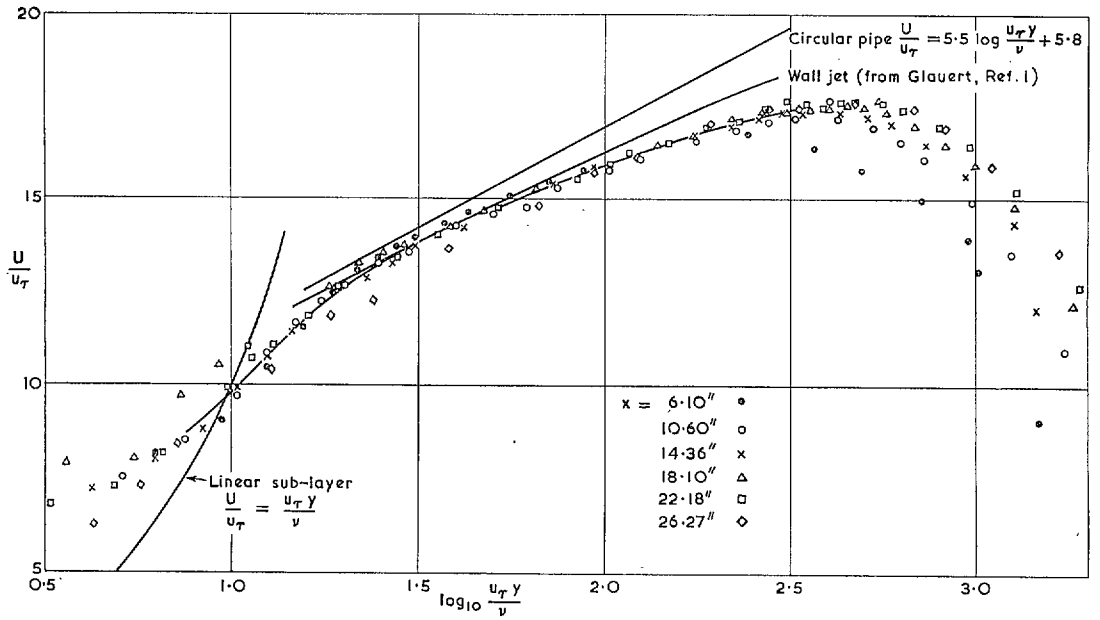

FIG. 6. Mean velocity profiles—wall jet in still air on flat surface—inner law plot.

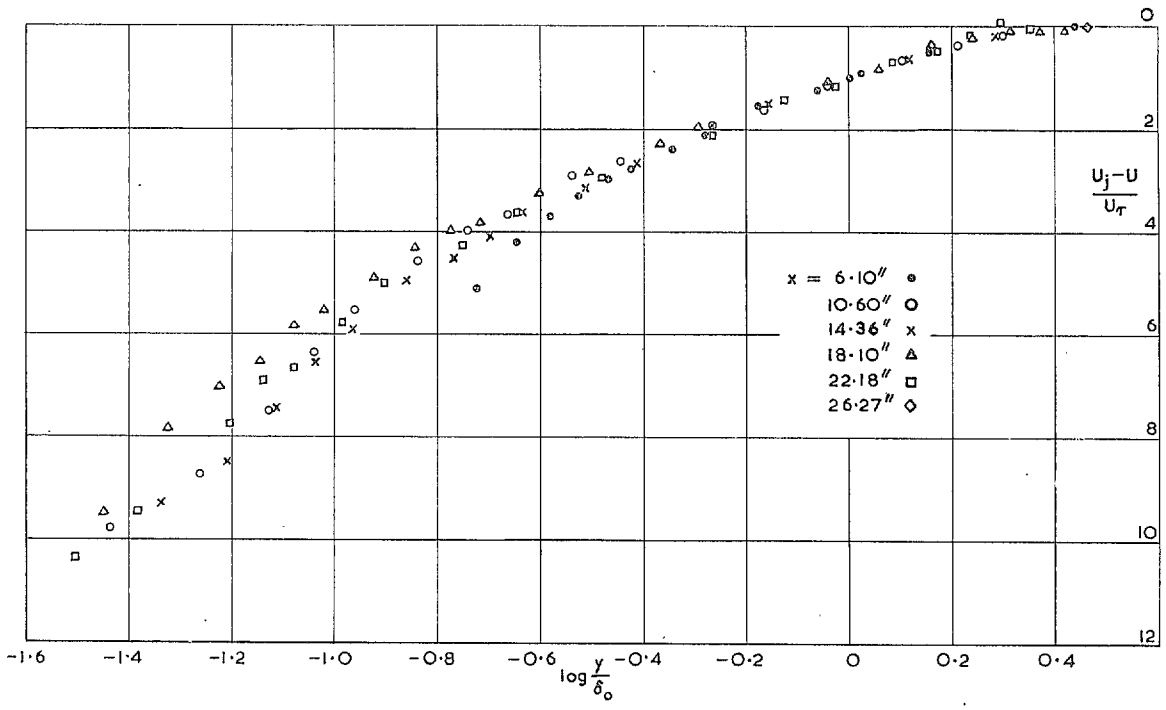

FIG. 7. Mean velocity profiles—wall jet in still air on flat surface—defect law plot.

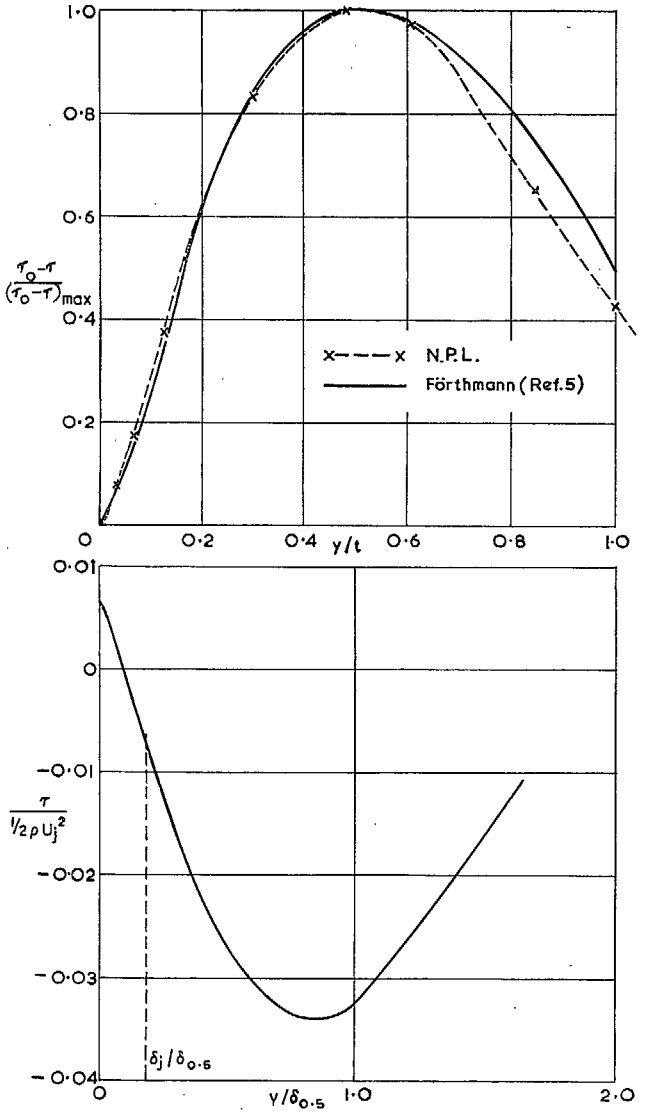

FIG. 8. Shear stress profile—wall jet in still air on flat surface.

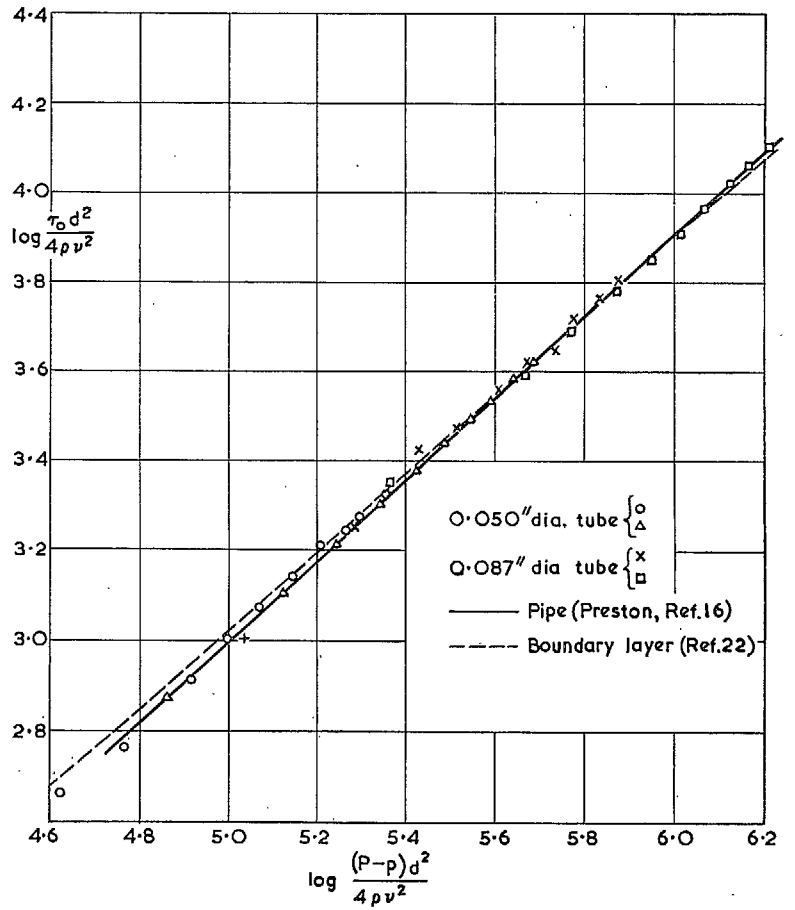

FIG. 9. Preston tube calibration—wall jet in still air on flat surface.

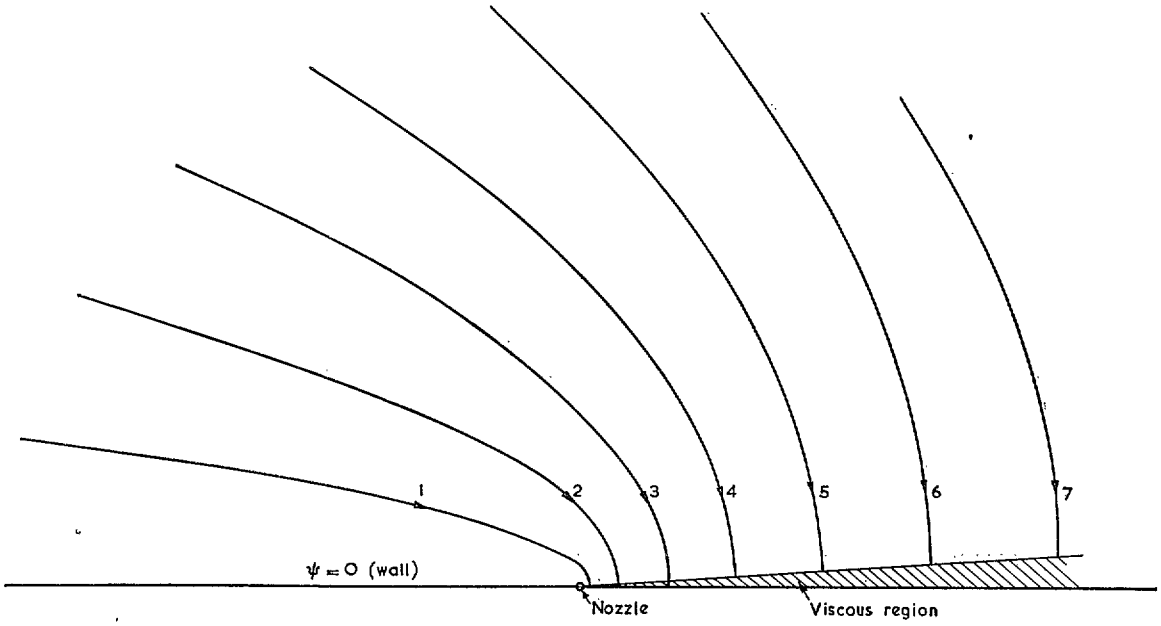

FIG. 10. Entrainment streamlines for free jet.

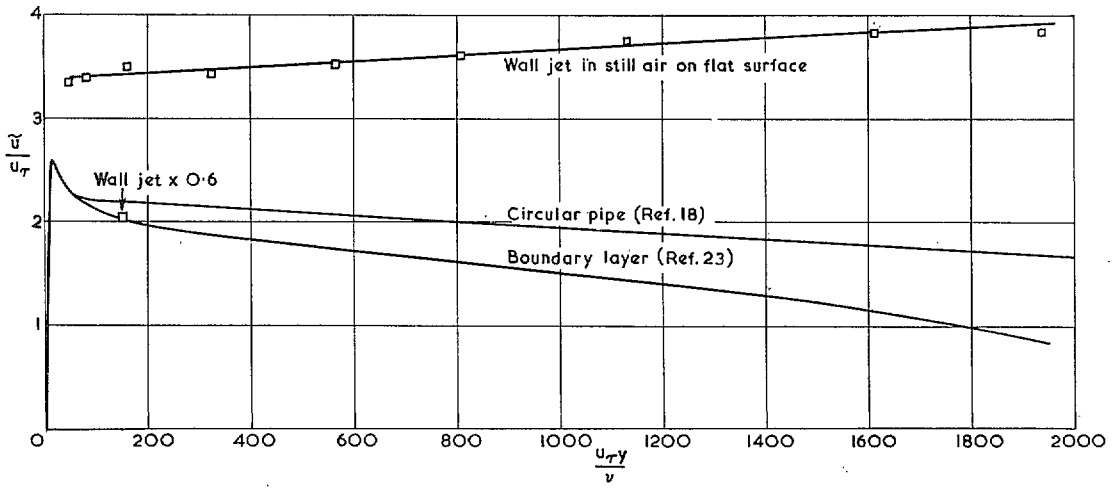

FIG. 11. Turbulent intensity profiles—circular pipe, boundary layer and wall jet in still air on flat surface.

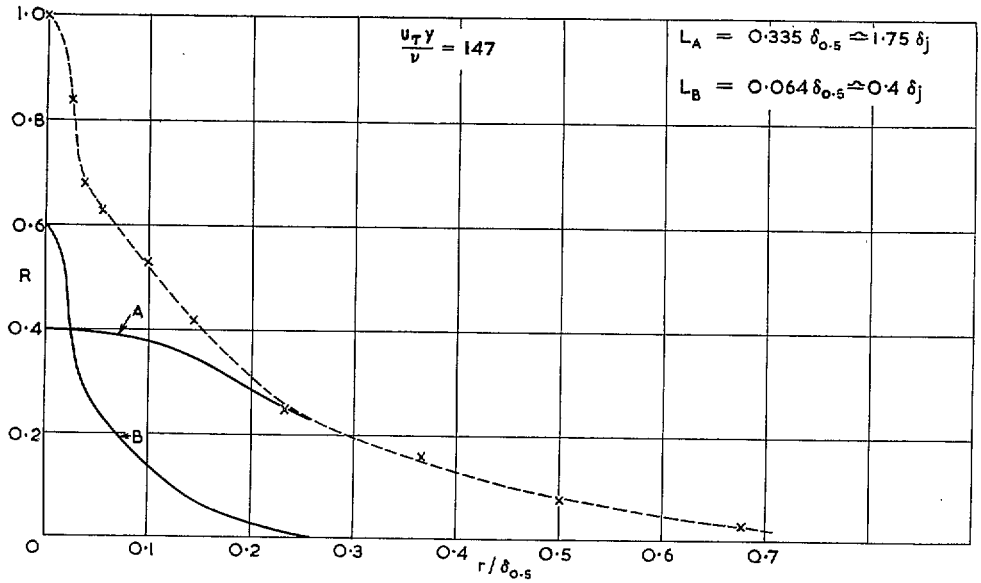

FIG. 12. R_{11} $(0{\cdot}042\delta_{0{\cdot}5} : o, r, o)$ correlation—wall jet in still air on flat surface.

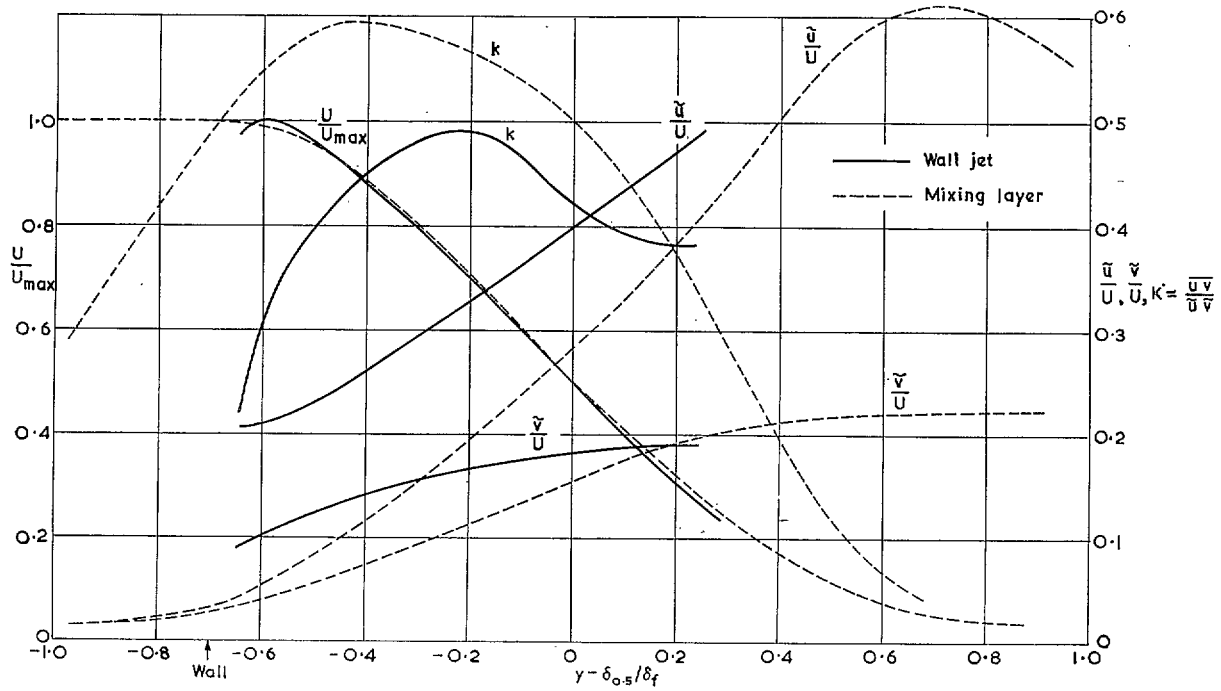

FIG. 13. Mean and turbulent velocity profiles—free mixing layer (Ref. 19) and wall jet in still air on flat surface.

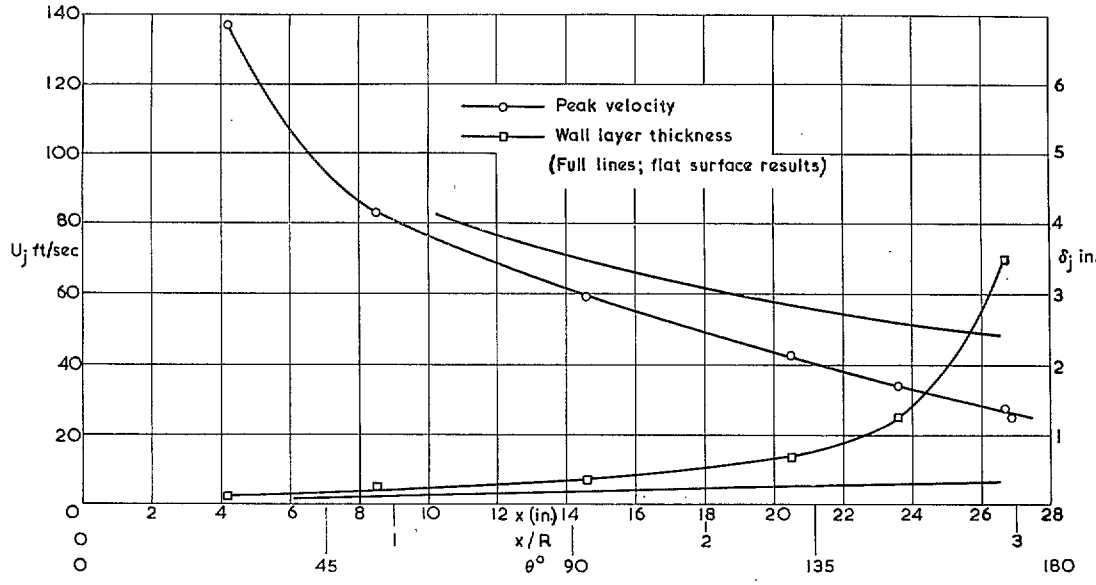

FIG. 14. Peak velocity and wall layer thickness—wall jet in still air on cylinder.

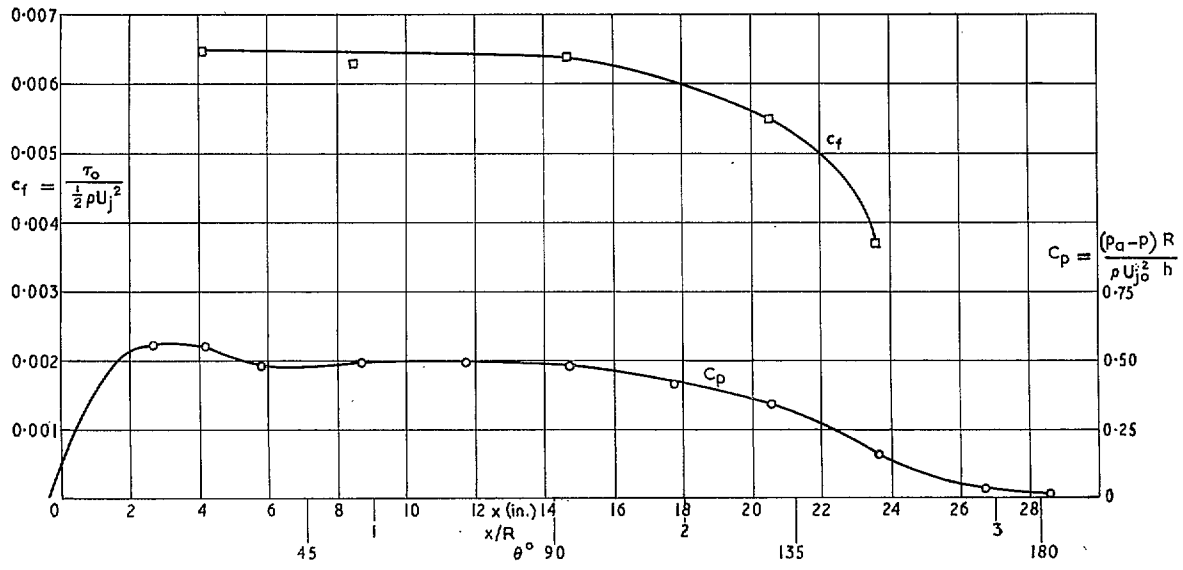

FIG. 15. Surface friction and surface pressure coefficients—wall jet in still air on cylinder.

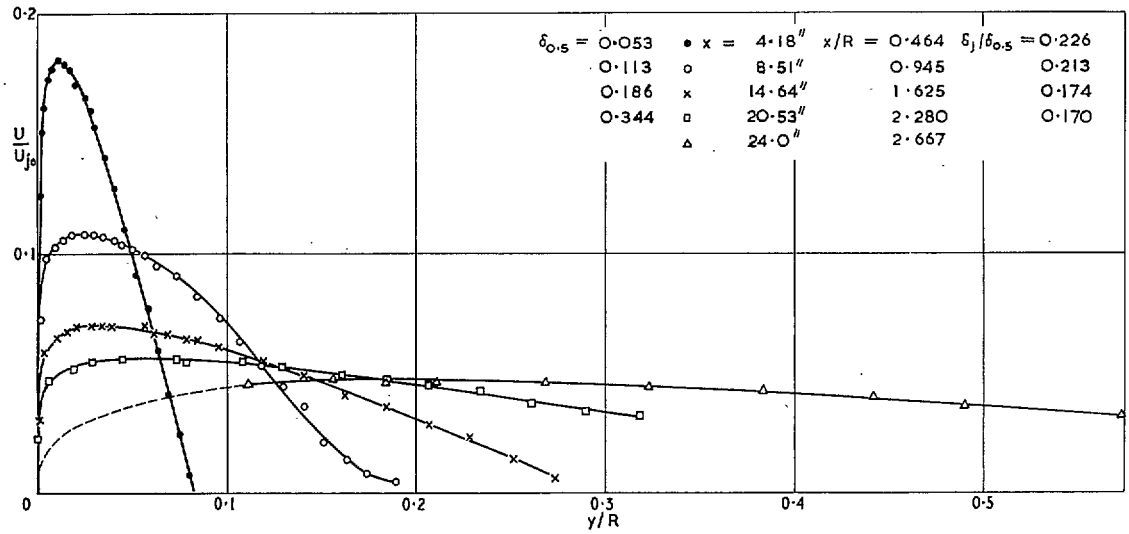

FIG. 16. Mean velocity profiles—wall jet in still air on cylinder.

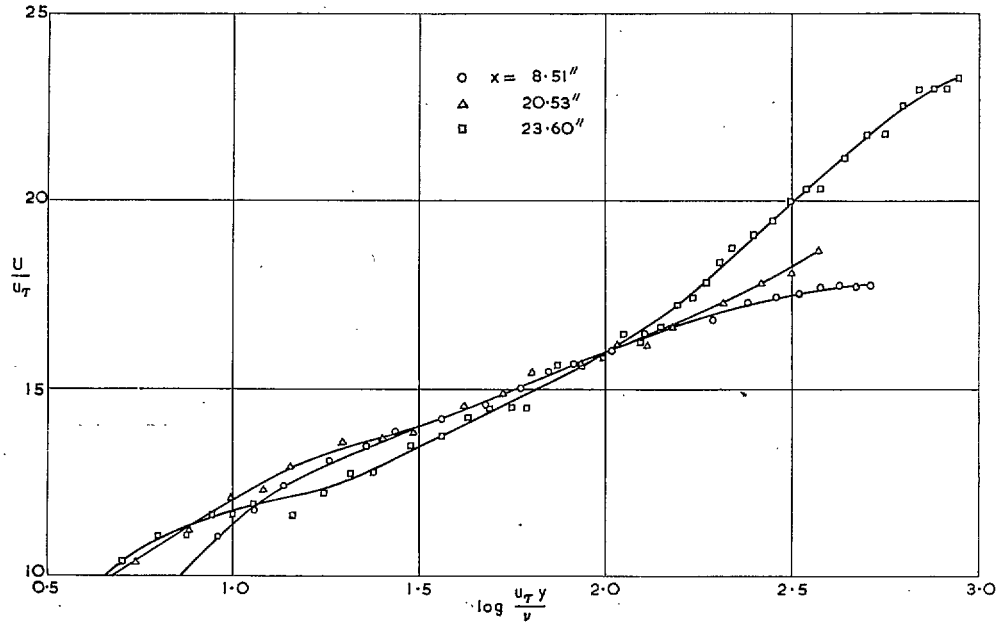

FIG. 17. Inner layer mean velocity profiles—wall jet in still air on cylinder—inner law plot.

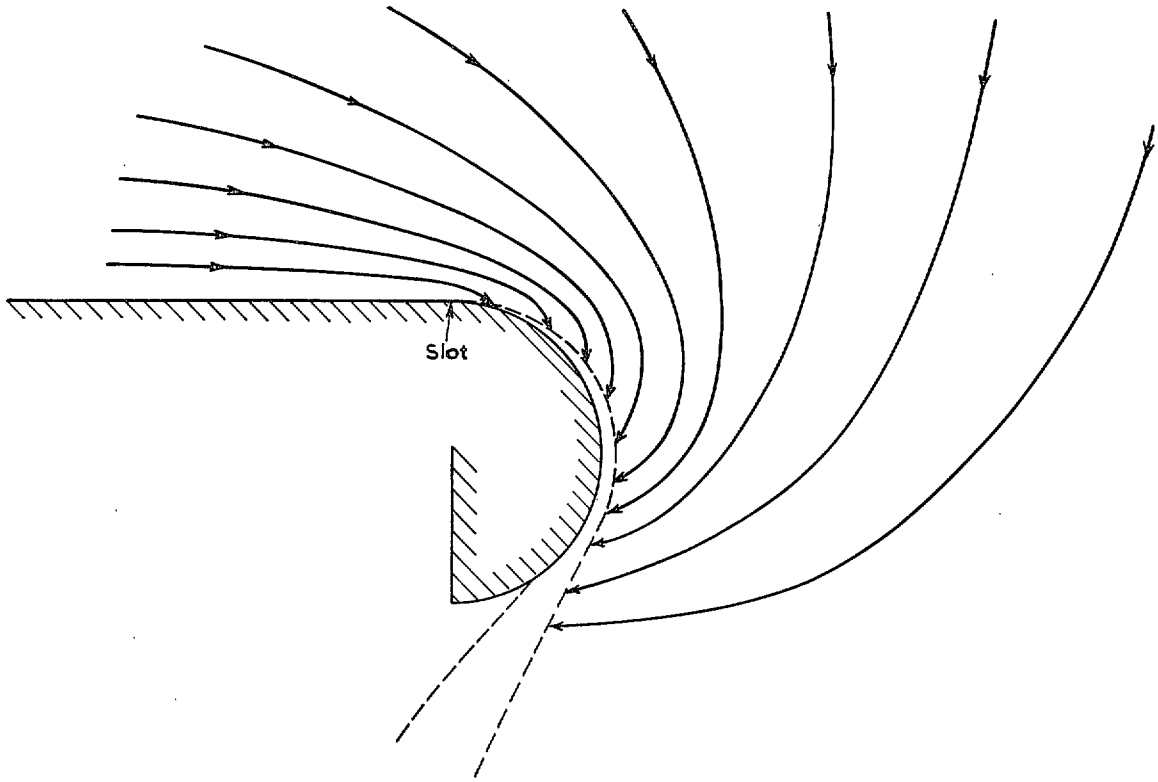

FIG. 18. Entrainment streamlines—wall jet in still air on cylinder (Not to scale).

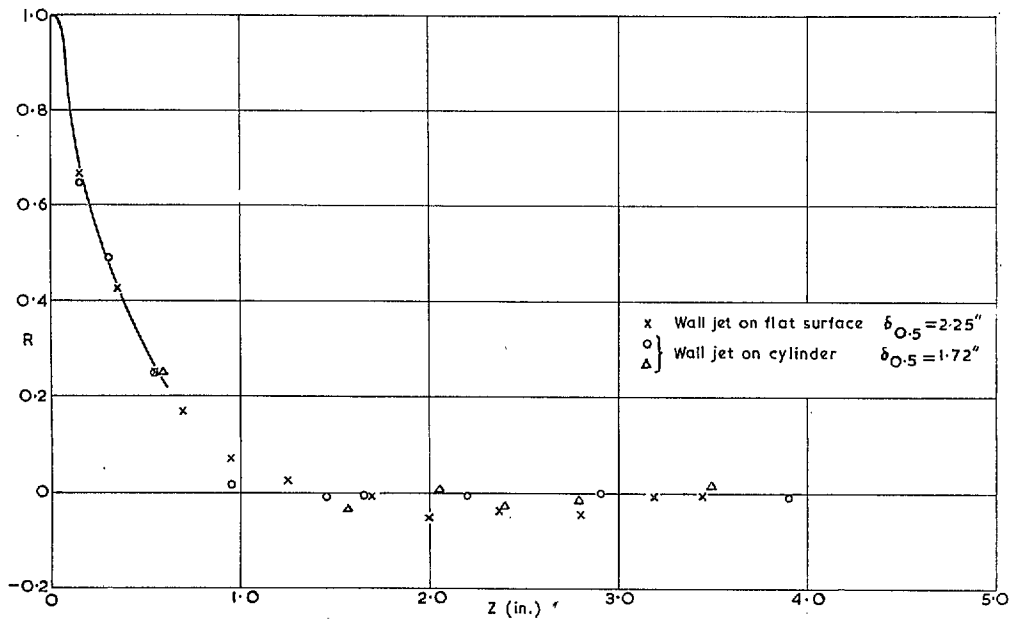

FIG. 19. $R_{22}(o, o, r)$ velocity correlations—wall jets in still air on flat surface and cylinder.

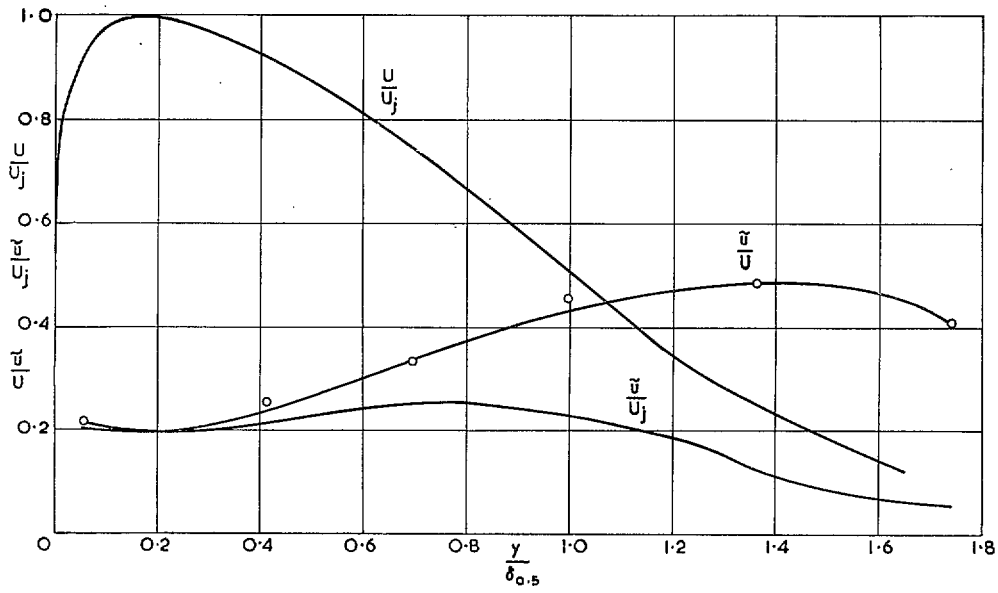

FIG. 20. Turbulence intensity profile—wall jet in still air on cylinder.

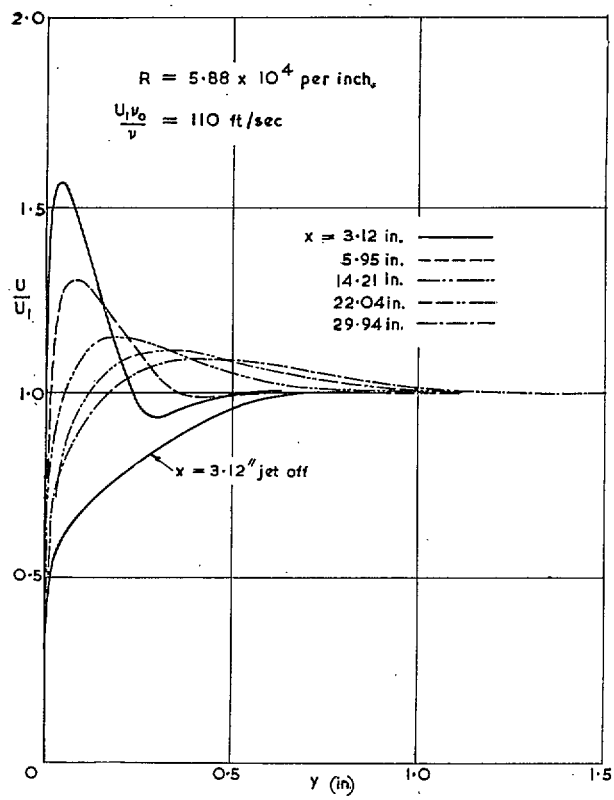

FIG. 21. Mean velocity profiles—wall jet beneath external stream in zero pressure gradient.

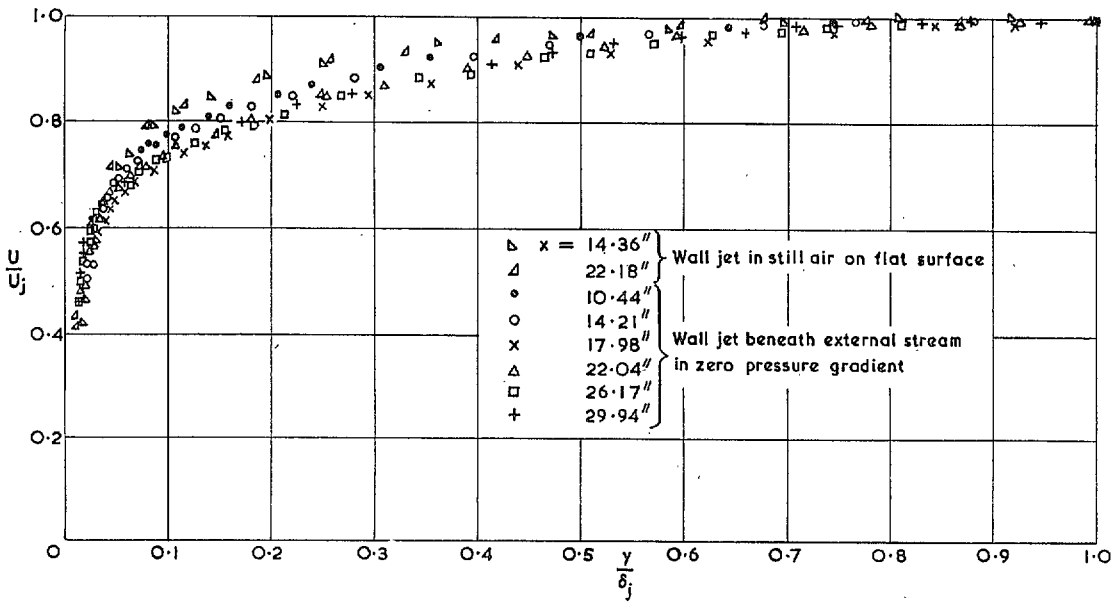

FIG. 22. Wall layer mean velocity profiles.

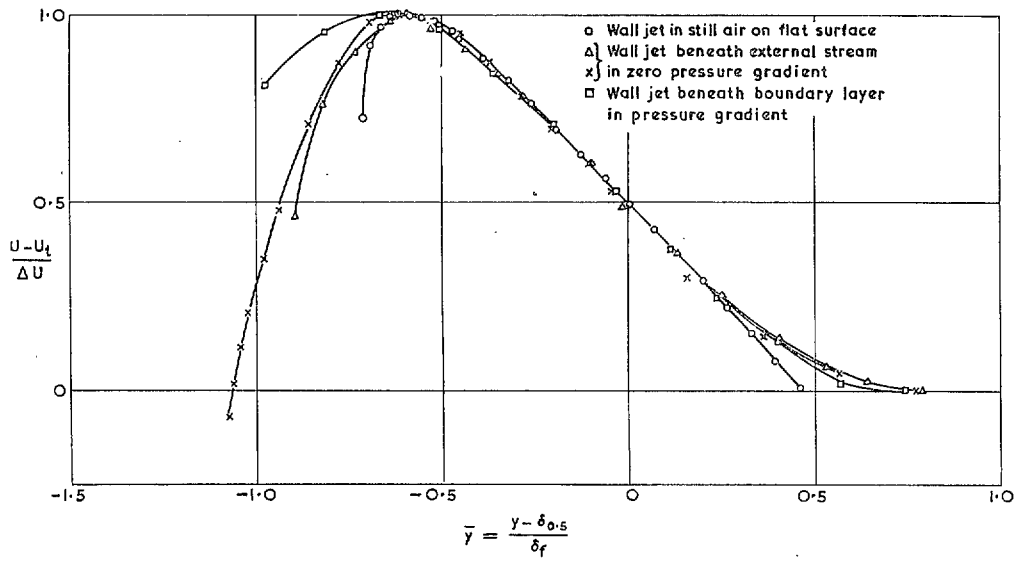

FIG. 23. Jet layer mean velocity profiles.

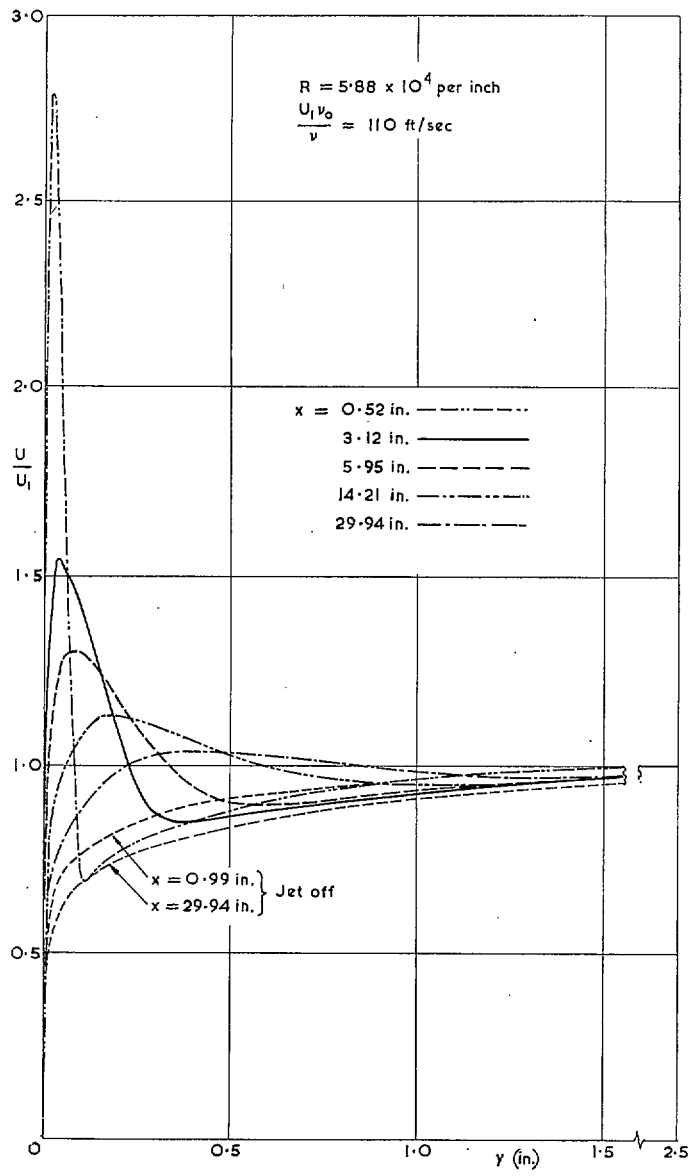

FIG. 24. Mean velocity profiles—wall jet beneath boundary layer in zero pressure gradient.

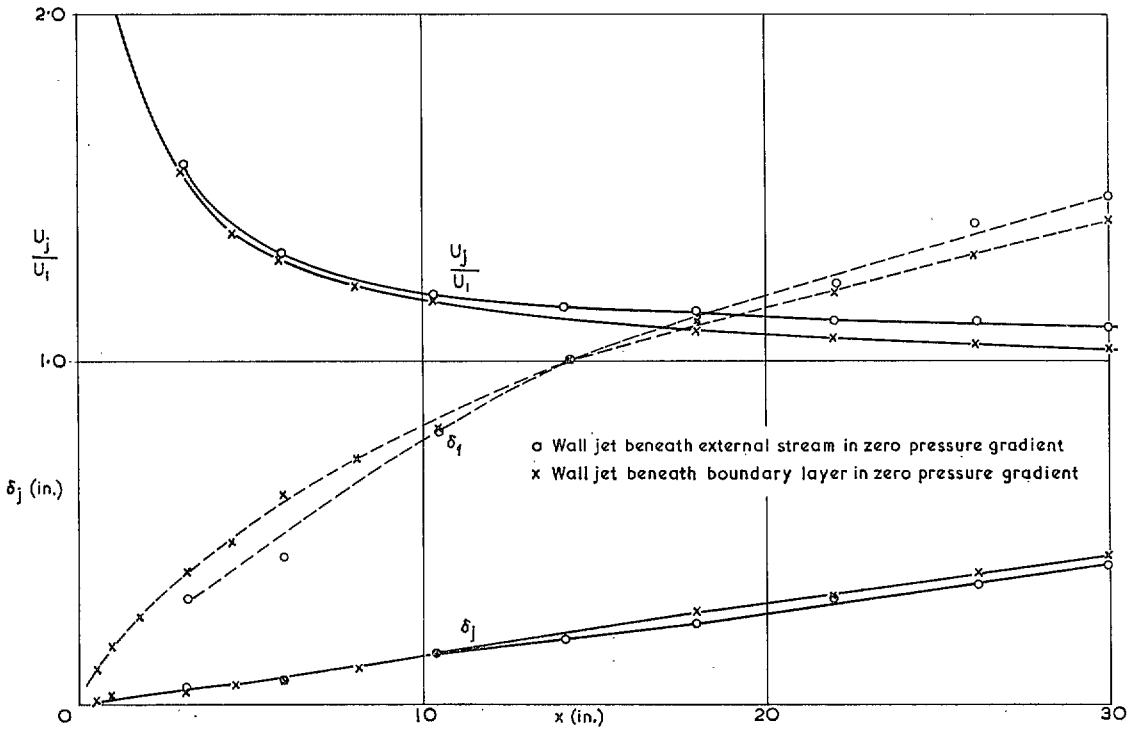

FIG. 25. Variation of layer thickness and maximum velocity—wall jet in zero pressure gradient.

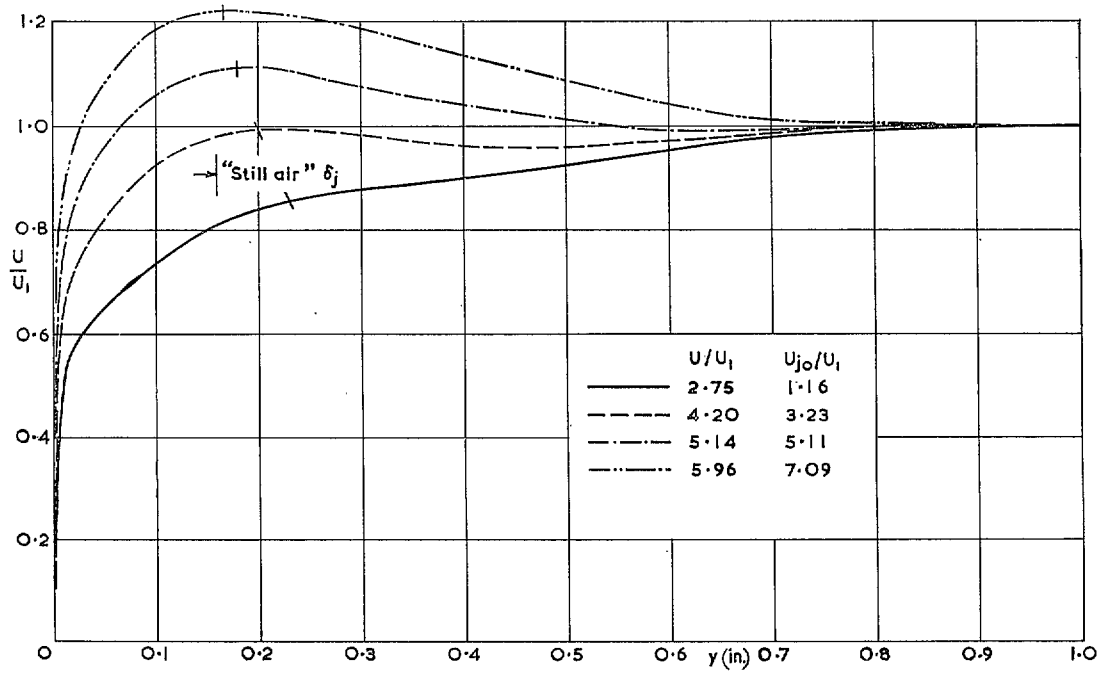

FIG. 26. Mean velocity profiles for varying U_{jo}—wall jet mixing with boundary layer in zero pressure gradient.

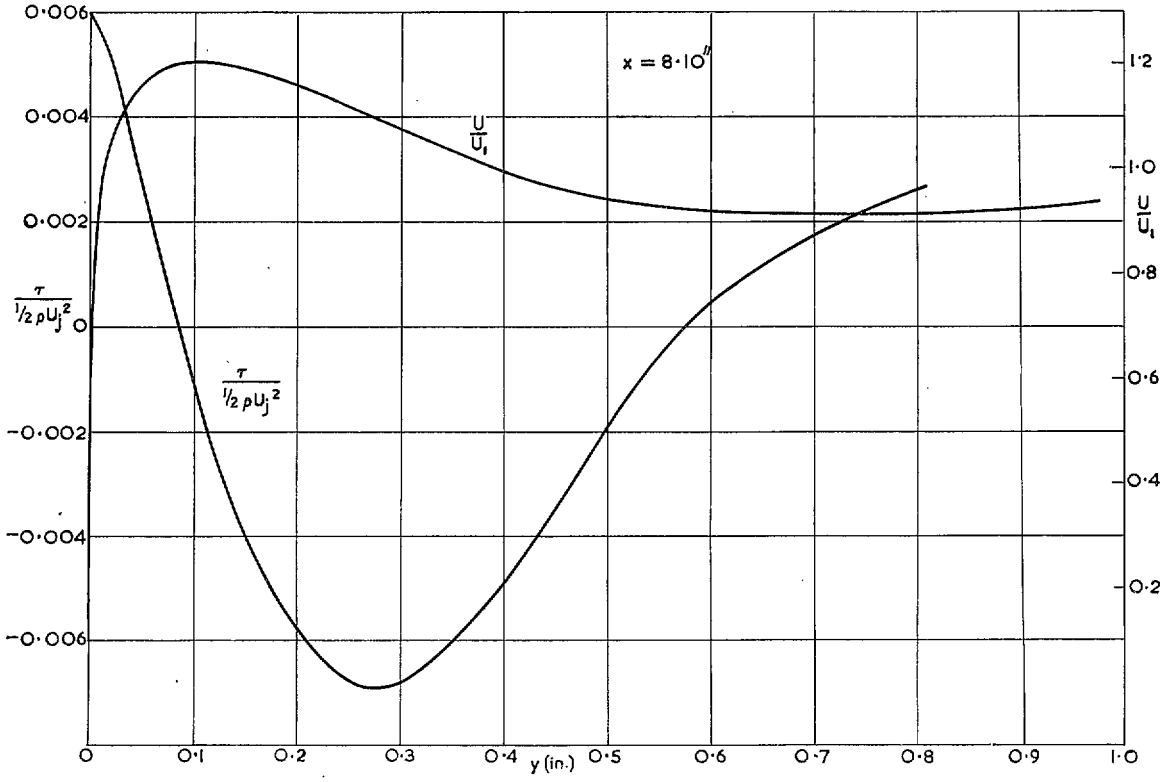

FIG. 27. Shear stress and mean velocity profiles—wall jet beneath boundary layer in zero pressure gradient.

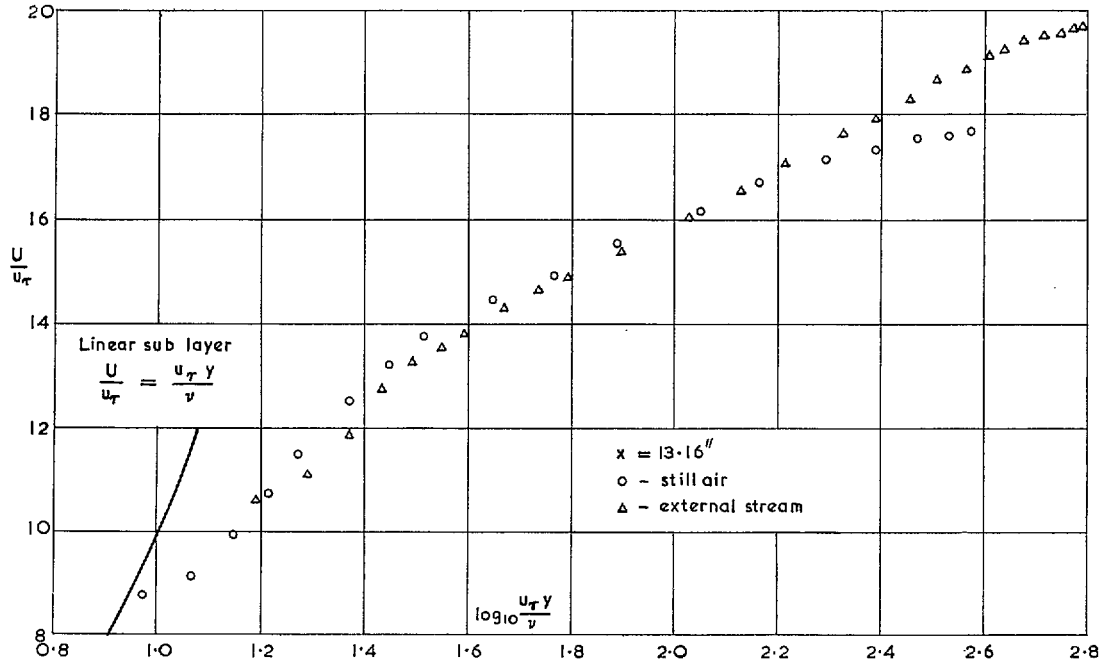

FIG. 28. Mean velocity profiles—wall jet in still air on flat surface and beneath an external stream in zero pressure gradient—inner law plot.

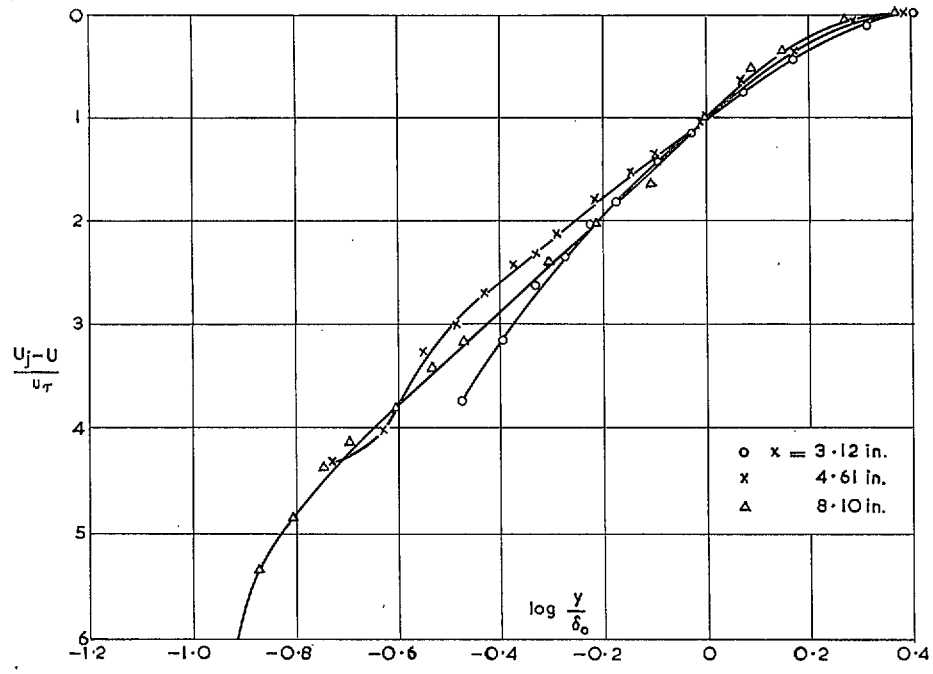

FIG. 29a. Wall layer mean velocity profiles—wall jet beneath free stream in zero pressure gradient—defect law plot.

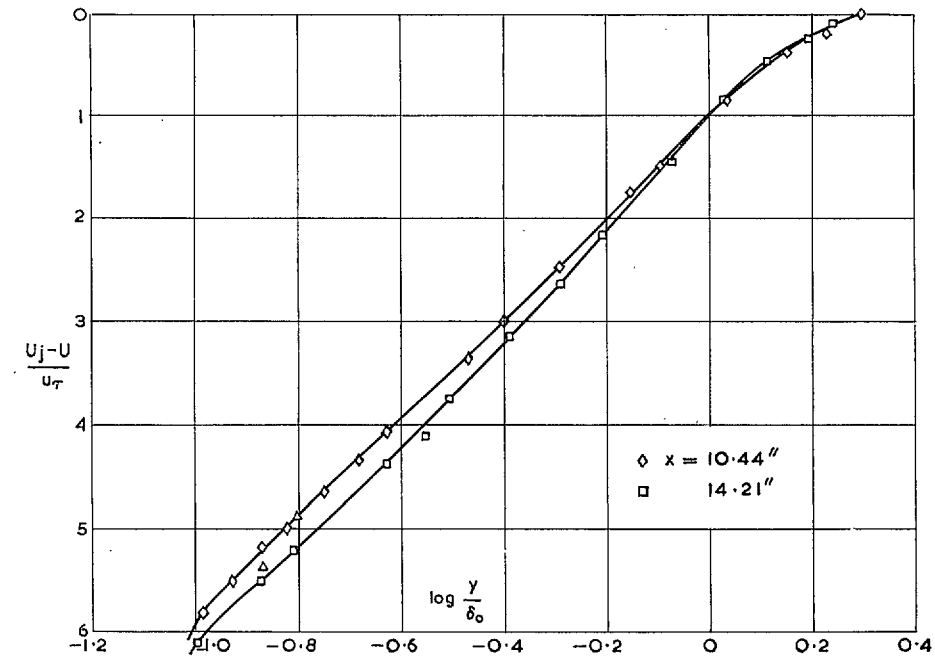

FIG. 29b. Defect law plot (*continued*).

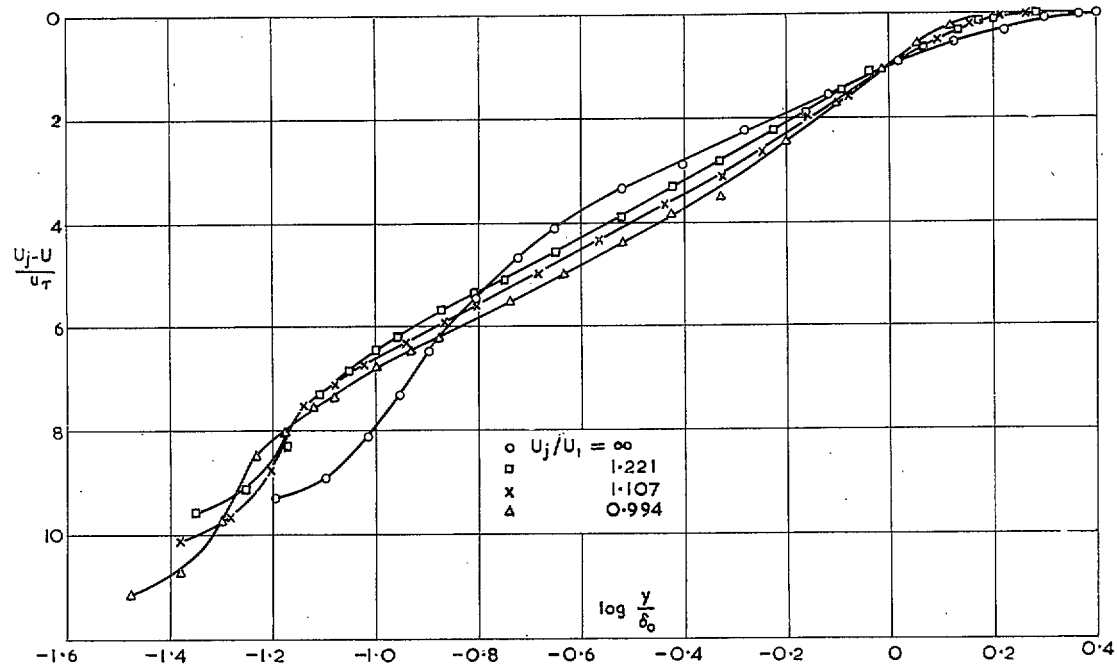

FIG. 29c. Mean velocity profiles—wall jet on flat surface—defect law plot.

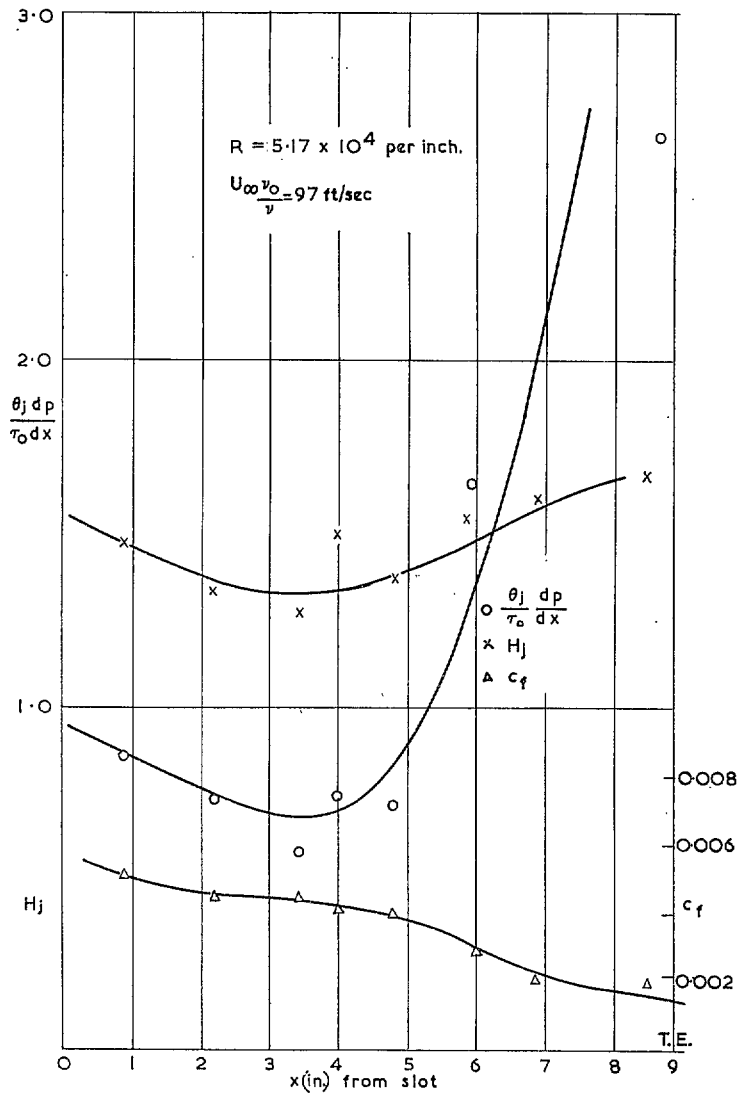

FIG. 30. Surface friction and equilibrium parameters—wall jet in pressure gradient.

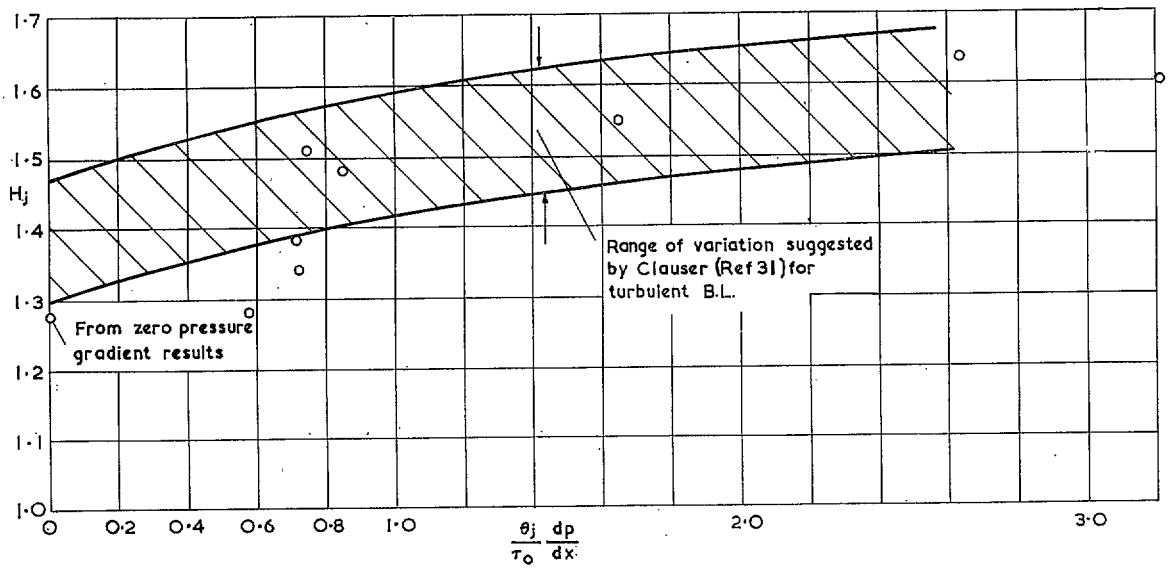

FIG. 31. Relation between shape parameters—wall jet in pressure gradient.

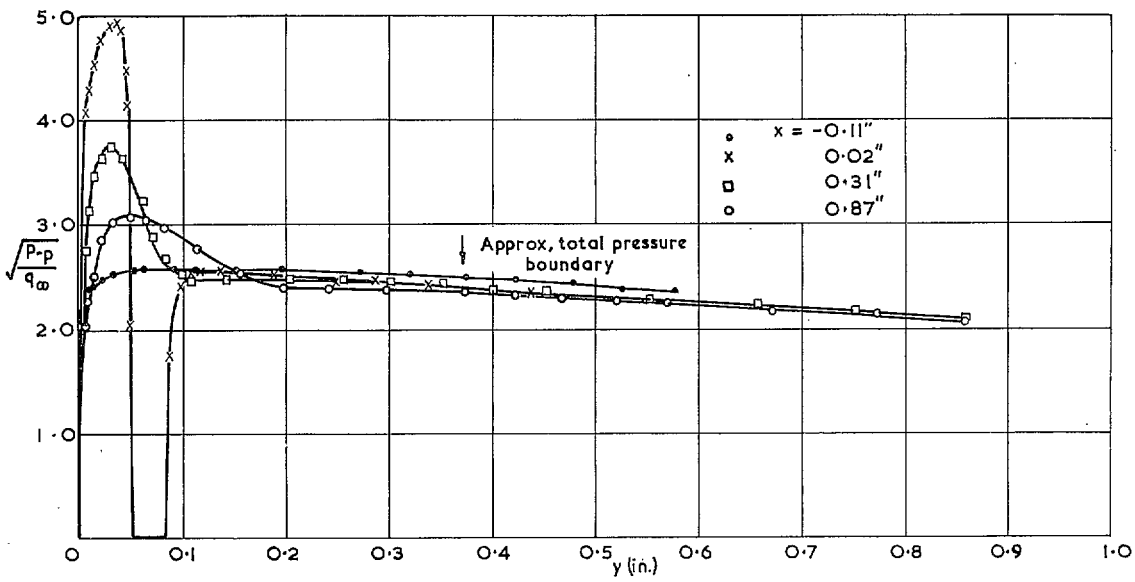

FIG. 32. Mean velocity profiles—wall jet in pressure gradient near knee of 46 deg deflected flap.

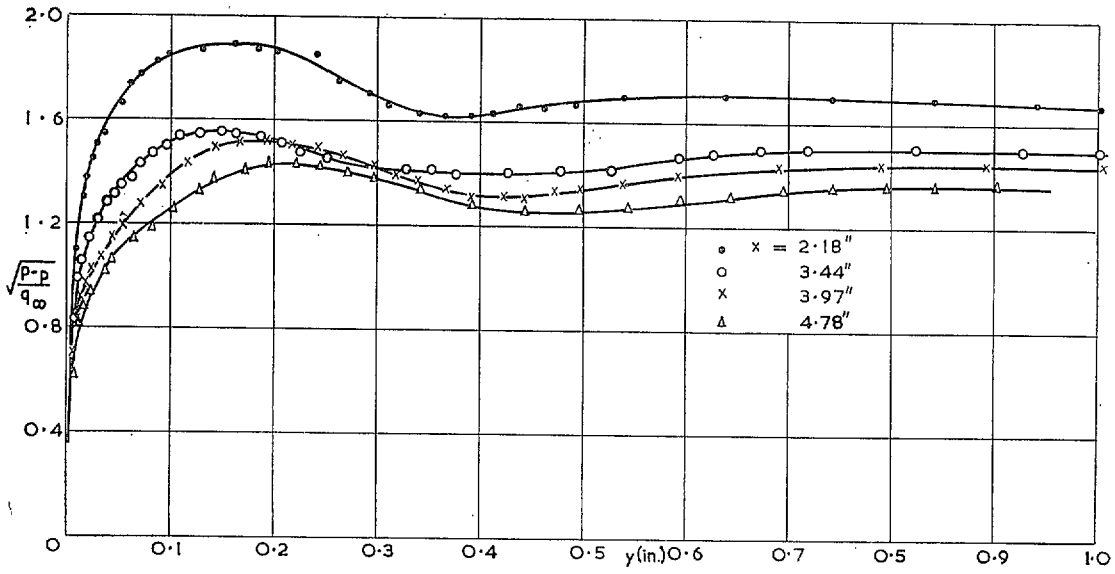

FIG. 33. Mean velocity profiles—wall jet in pressure gradient—straight portion of flap.

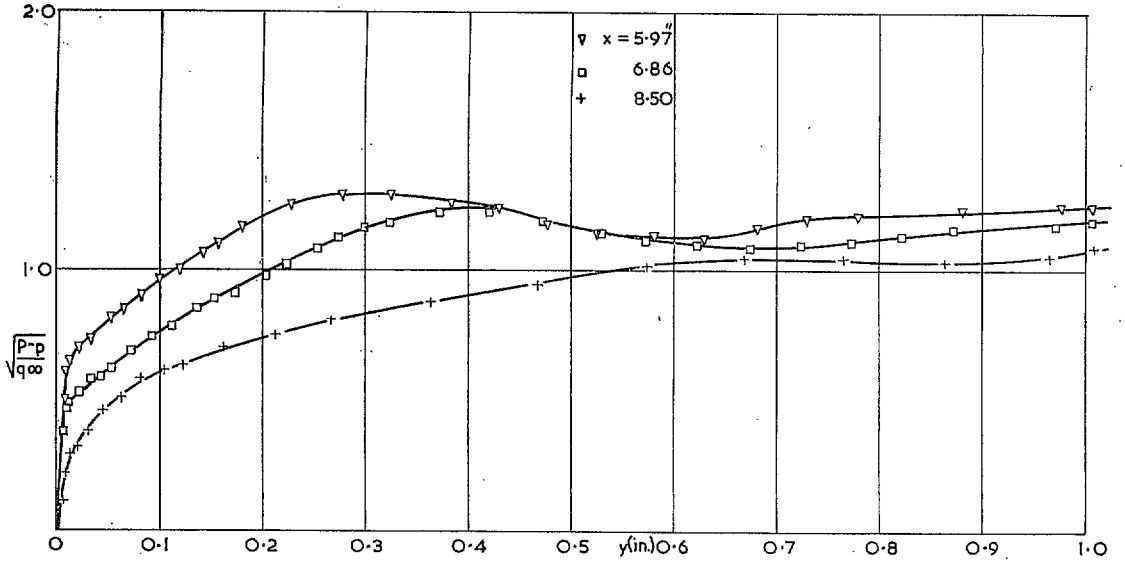

FIG. 34. Mean velocity profiles—wall jet in pressure gradient near trailing edge of flap.

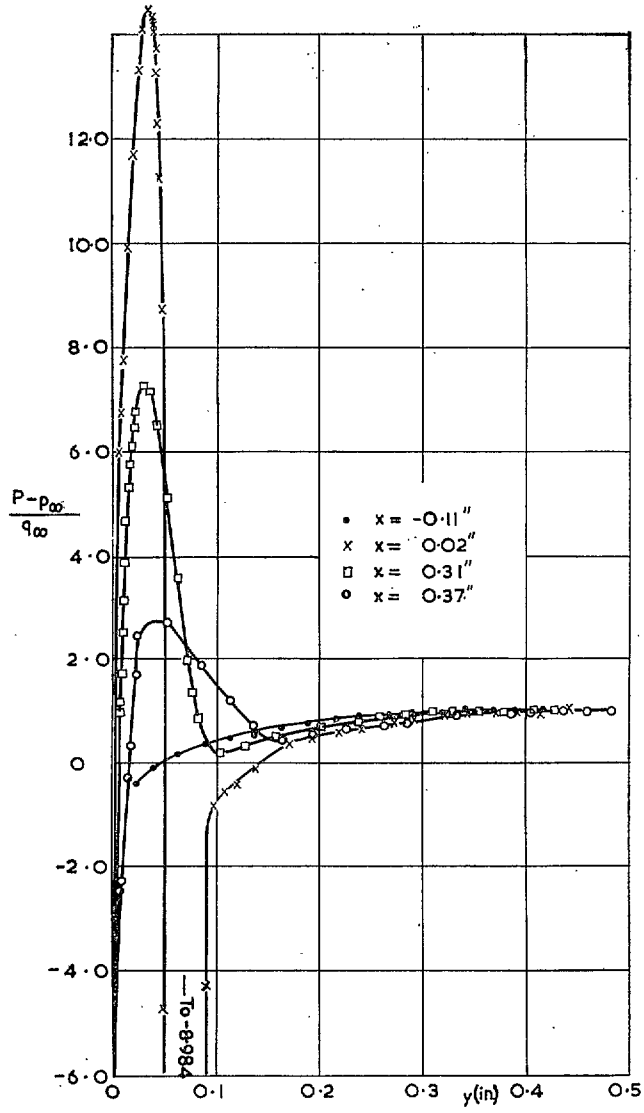

FIG. 35. Total pressure profiles near slot—wall jet in pressure gradient.

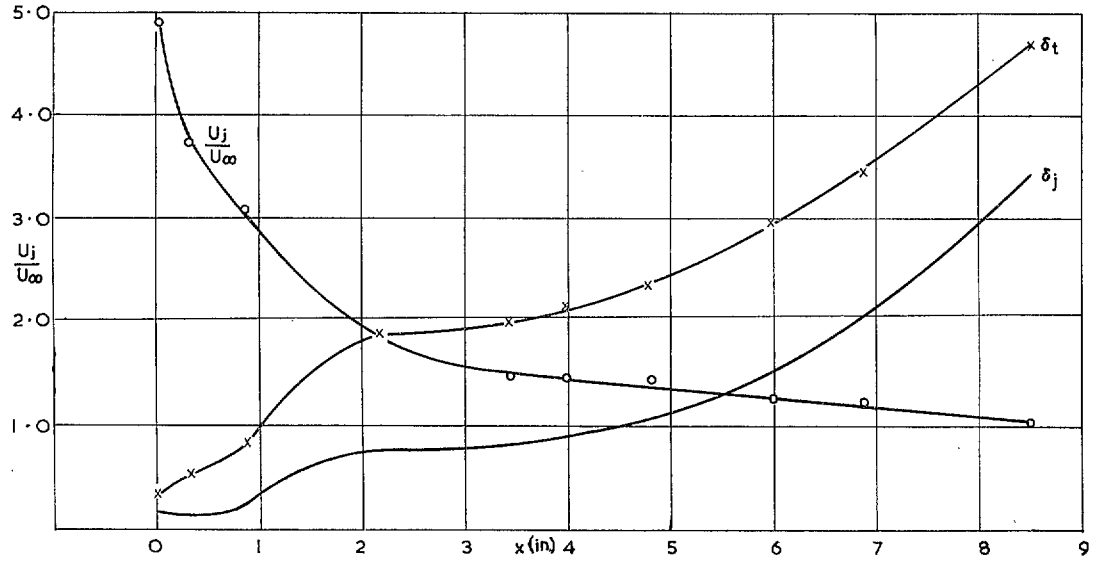

FIG. 36. Variation of layer thickness and maximum velocity—wall jet in pressure gradient.

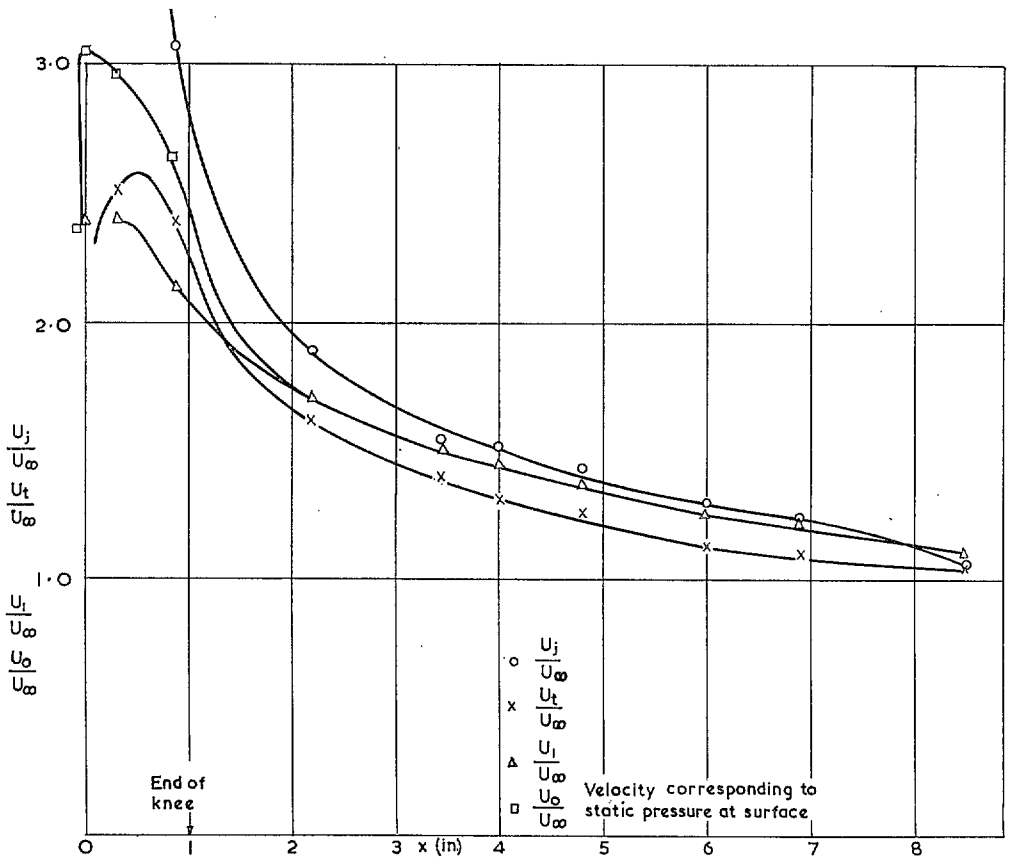

FIG. 37. Variation of peak, trough and free-stream velocities—wall jet in pressure gradient.

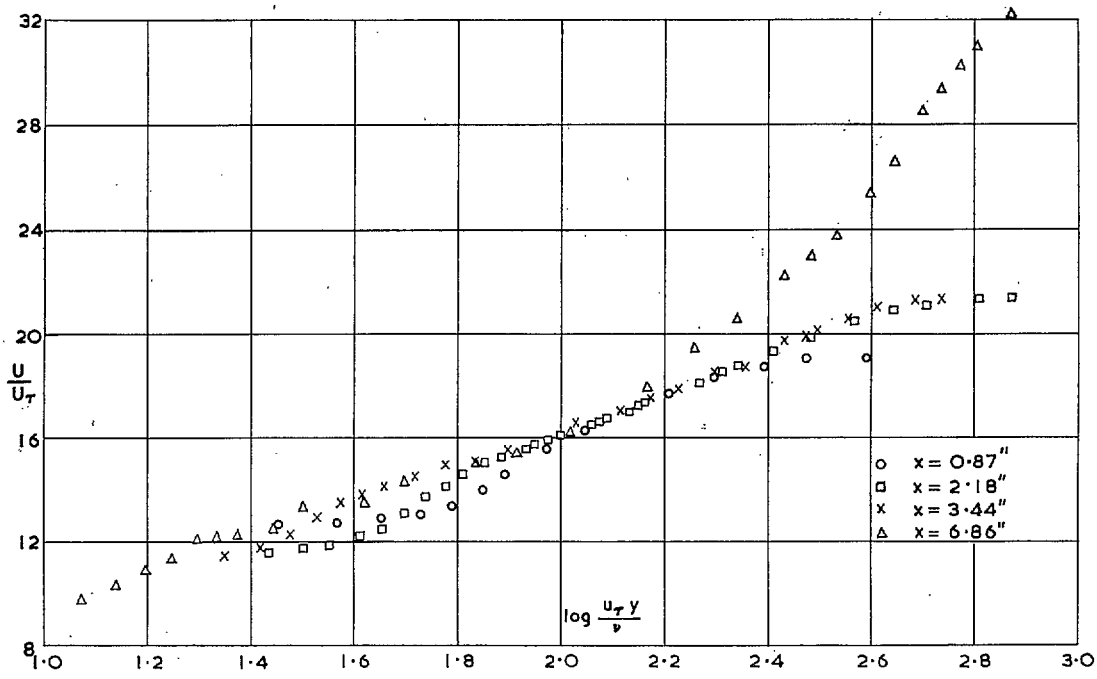

FIG. 38. Mean velocity profiles—wall jet in pressure gradient—inner law plot.

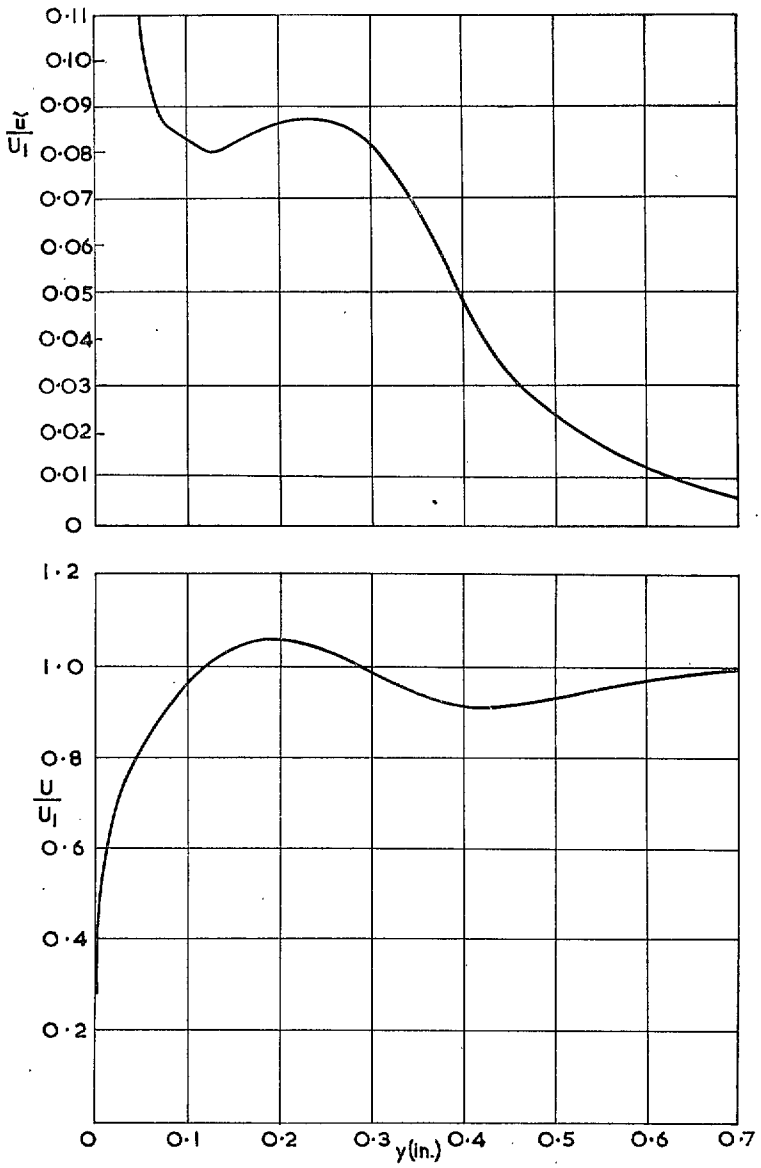

FIG. 39. Turbulent intensity and corresponding mean velocity profile—wall jet in pressure gradient. Traverse 3·97 in. aft of slot.

(83534) Wt. 67/1876 K.5 1/62 Hw.

Publications of the Aeronautical Research Council

ANNUAL TECHNICAL REPORTS OF THE AERONAUTICAL RESEARCH COUNCIL (BOUND VOLUMES)

1941 Aero and Hydrodynamics, Aerofoils, Airscrews, Engines, Flutter, Stability and Control, Structures. 63*s.* (post 2*s.* 3*d.*)

1942 Vol. I. Aero and Hydrodynamics, Aerofoils, Airscrews, Engines. 75*s.* (post 2*s.* 3*d.*)
Vol. II. Noise, Parachutes, Stability and Control, Structures, Vibration, Wind Tunnels. 47*s.* 6*d.* (post 1*s.* 9*d.*)

1943 Vol. I. Aerodynamics, Aerofoils, Airscrews. 80*s.* (post 2*s.*)
Vol. II. Engines, Flutter, Materials, Parachutes, Performance, Stability and Control, Structures. 90*s.* (post 2*s.* 3*d.*)

1944 Vol. I. Aero and Hydrodynamics, Aerofoils, Aircraft, Airscrews, Controls. 84*s.* (post 2*s.* 6*d.*)
Vol. II. Flutter and Vibration, Materials, Miscellaneous, Navigation, Parachutes, Performance, Plates and Panels, Stability, Structures, Test Equipment, Wind Tunnels. 84*s.* (post 2*s.* 6*d.*)

1945 Vol. I. Aero and Hydrodynamics, Aerofoils. 130*s.* (post 3*s.*)
Vol. II. Aircraft, Airscrews, Controls. 130*s.* (post 3*s.*)
Vol. III. Flutter and Vibration, Instruments, Miscellaneous, Parachutes, Plates and Panels, Propulsion. 130*s.* (post 2*s.* 9*d.*)
Vol. IV. Stability, Structures, Wind Tunnels, Wind Tunnel Technique. 130*s.* (post 2*s.* 9*d.*)

1946 Vol. I. Accidents, Aerodynamics, Aerofoils and Hydrofoils. 168*s.* (post 3*s.* 3*d.*)
Vol. II. Airscrews, Cabin Cooling, Chemical Hazards, Controls, Flames, Flutter, Helicopters, Instruments and Instrumentation, Interference, Jets, Miscellaneous, Parachutes. 168s. (post 2*s.* 9*d.*)
Vol. III. Performance, Propulsion, Seaplanes, Stability, Structures, Wind Tunnels. 168*s.* (post 3*s.*)

1947 Vol. I. Aerodynamics, Aerofoils, Aircraft. 168*s.* (post 3*s.* 3*d.*)
Vol. II. Airscrews and Rotors, Controls, Flutter, Materials, Miscellaneous, Parachutes, Propulsion, Seaplanes, Stability, Structures, Take-off and Landing. 168*s.* (post 3*s.* 3*d.*)

Special Volumes

Vol. I. Aero and Hydrodynamics, Aerofoils, Controls, Flutter, Kites, Parachutes, Performance, Propulsion, Stability. 126*s.* (post 2*s.* 6*d.*)
Vol. II. Aero and Hydrodynamics, Aerofoils, Airscrews, Controls, Flutter, Materials, Miscellaneous, Parachutes, Propulsion, Stability, Structures. 147*s.* (post 2*s.* 6*d.*)
Vol. III. Aero and Hydrodynamics, Aerofoils, Airscrews, Controls, Flutter, Kites, Miscellaneous, Parachutes, Propulsion, Seaplanes, Stability, Structures, Test Equipment. 189*s.* (post 3*s.* 3*d.*)

Reviews of the Aeronautical Research Council

1939–48 3*s.* (post 5*d.*) 1949–54 5*s.* (post 5*d.*)

Index to all Reports and Memoranda published in the Annual Technical Reports

1909–1947 R. & M. 2600 6*s.* (post 2*d.*)

Indexes to the Reports and Memoranda of the Aeronautical Research Council

Between Nos. 2351–2449	R. & M. No. 2450 2*s.* (post 2*d.*)
Between Nos. 2451–2549	R. & M. No. 2550 2*s.* 6*d.* (post 2*d.*)
Between Nos. 2551–2649	R. & M. No. 2650 2*s.* 6*d.* (post 2*d.*)
Between Nos. 2651–2749	R. & M. No. 2750 2*s.* 6*d.* (post 2*d.*)
Between Nos. 2751–2849	R. & M. No. 2850 2*s.* 6*d.* (post 2*d.*)
Between Nos. 2851–2949	R. & M. No. 2950 3*s.* (post 2*d.*)
Between Nos. 2951–3049	R. & M. No. 3050 3*s.* 6*d.* (post 2*d.*)

HER MAJESTY'S STATIONERY OFFICE

from the addresses overleaf

Printed and published by
HER MAJESTY'S STATIONERY OFFICE

To be purchased from
York House, Kingsway, London W.C.2
423 Oxford Street, London W.1
13A Castle Street, Edinburgh 2
109 St. Mary Street, Cardiff
39 King Street, Manchester 2
50 Fairfax Street, Bristol 1
2 Edmund Street, Birmingham 3
80 Chichester Street, Belfast 1
or through any bookseller

Printed in England

S.O. Code No. 23-3252